

General Disclaimer

One or more of the Following Statements may affect this Document

- This document has been reproduced from the best copy furnished by the organizational source. It is being released in the interest of making available as much information as possible.
- This document may contain data, which exceeds the sheet parameters. It was furnished in this condition by the organizational source and is the best copy available.
- This document may contain tone-on-tone or color graphs, charts and/or pictures, which have been reproduced in black and white.
- This document is paginated as submitted by the original source.
- Portions of this document are not fully legible due to the historical nature of some of the material. However, it is the best reproduction available from the original submission.

Reports of the Department of Geodetic Science and Surveying

Report No. 327

ALTERNATIVE METHODS TO SMOOTH THE EARTH'S GRAVITY FIELD

by

Christopher Jekeli

(NASA-CR-168758) ALTERNATIVE METHODS TO
SMOOTH THE EARTH'S GRAVITY FIELD (Ohio State
Univ., Columbus.) 53 p HC AC4/MF A01

N82-22821

CSSL 08G

Unclas

G3/46 09551

Prepared for

National Aeronautics and Space Administration
Goddard Space Flight Center
Greenbelt, Maryland 20770

Grant No. NGR36-008-161
OSURF Project 783210



The Ohio State University
Department of Geodetic Science and Surveying
1958 Neil Avenue
Columbus, Ohio 43210

December, 1981

Abstract

Convolutions on the sphere with corresponding convolution theorems are developed for one- and two-dimensional functions. Some of these results are used in a study of isotropic smoothing operators or filters. Well known filters in Fourier spectral analysis, such as the rectangular, Gaussian, and Hanning filters, are adapted for data on a sphere. The low-pass filter most often used on gravity data is the rectangular (or Pellinen) filter. However, its spectrum has relatively large sidelobes; and therefore, this filter passes a considerable part of the upper end of the gravity spectrum. The spherical adaptations of the Gaussian and Hanning filters are more efficient in suppressing the high-frequency components of the gravity field since their frequency response functions are strongly tapered at the high frequencies with no, or small, sidelobes. Formulas are given for practical implementation of these "new" filters, including a demonstration that the large negative sidelobe of the Pellinen response can cause 180° shifts in the smoothed function.

Foreword

This report was prepared by Christopher Jekeli, Graduate Research Associate, the Department of Geodetic Science and Surveying, The Ohio State University. This research was supported, in part, under NASA Grant NGR36-008-161, The Ohio State University Research Foundation Project 783210. The grant covering this research is administered through the NASA Goddard Space Flight Center, Greenbelt, Maryland, Mr. Jean Welker, Technical Officer.

Acknowledgements

I am very grateful to my advisor, Dr. Richard H. Rapp, for his continued support during the course of this work. Also, many thanks go to Susan Carroll for the excellent typing of the draft. Computer time for the numerical computations was generously provided by the Instruction and Research Computer Center of The Ohio State University.

Table of Contents

	Page
1. Introduction.	1
2. Convolutions on the Sphere.	1
3. The Mean Gravity Anomaly.	13
3.1 The Pellinen Mean	15
3.2 The Gaussian Mean	17
3.3 The Hanning Mean	24
3.4 The Upward Continuation (Poisson) Operator. .	25
3.5 The Ideal Filter.	26
3.6 Discrete Operators.	27
4. Smoothing a Simulated Gravity Field	28
5. Conclusion.	41
References.	44
Appendix A.	46
Appendix B.	46

1. Introduction

To the statistician the word "mean" denotes the value to be expected when sampling a given population of values. Statistically, the expected value is nothing more than one of several constant parameters that describe the population. When the geodesist speaks of a mean gravity anomaly (or mean geoid undulation) he does not consider the entire terrestrial population of gravity anomalies, and yet it serves as a consistent descriptor of the earth's gravity field. The mean gravity anomaly is, in the most general terms, defined as the (possibly weighted) average of a subpopulation of anomalies distributed over a particular region of the earth's surface, for example, over a block delimited by pairs of latitude and longitude lines. The total number of regions of a given size which together form the earth's surface is finite, but there exists an infinite number of ways to partition the surface into regions of one size (for example, by simply changing the location of the zero meridian). Consequently, the set of corresponding mean anomalies (the "moving average") forms a new infinite population which reflects the characteristics of the total gravity field to some degree of detail. It describes a field that, more or less, is a generalization of the actual field, representing the dominant or essential features and suppressing unnecessary or unwanted details.

The following mathematical treatment sets the stage for the study of the different weighting schemes that can be used to define the mean gravity anomaly, thus making the above loose statements more rigorous. This can be accomplished effectively only by representing the gravity anomaly in terms of its spectrum, which is the set of coefficients in its representation by a series of spherical harmonic functions. This definition of the spectrum necessitates the approximation of the earth's surface by a sphere only if the spectra of the terrestrial anomaly and the anomaly on a sphere external to the earth (e.g. for satellite applications) are to be consistent. Otherwise, a spectrum is definable for any surface, approximating the earth, that can be mapped onto the unit sphere using a one-to-one correspondence. The gravity anomaly enters the discussion only as an example, since any of the geodetic quantities, indeed any function that is expandable in spherical harmonics, would serve equally well.

2. Convolutions on the Sphere

The first part of this paper shows how several concepts of spectral theory common in electrical engineering and communication theory can be applied and understood in physical geodesy (see also Robertson, 1978; Kaula, 1959, 1967). The

subsequent formulas by themselves are not new in geodesy, however they are viewed from the standpoint of spectral theory which acts to unify several diverse areas of physical geodesy.

Since geodetic data pertaining to the gravity field are obtained either on the earth's surface (approximately spherical) or by earth-orbiting satellites (approximately circular orbits), it becomes computationally expedient to consider functions in terms of spherical coordinates. Note, however, that for certain local studies the plane may serve as a sufficient approximation of the earth's surface, in which case two-or three-dimensional Cartesian coordinates are more appropriate (Moritz, 1966; Rayner, 1971; Breakwell, 1979; see also Jordan (1978) who develops an interesting synthesis of the global and local situations). The Cartesian coordinates are particularly attractive due to the ease with which the Fourier transforms can be computed.

Let $F(\theta, \lambda)$ be a function defined on the unit sphere (the scale of the sphere is immaterial). θ , λ are the usual spherical coordinates, being respectively the polar angle (colatitude) and the longitude. In analogy to the familiar Fourier transform, applicable to functions defined in rectangular coordinates, we define the two-dimensional "Legendre transform" as

$$L_2[F] = \frac{1}{4\pi} \iint_{\sigma} F(\theta, \lambda) \bar{Y}_{nm}(\theta, \lambda) d\sigma = f_{nm}, \quad (1)$$

where σ represents the unit sphere ($0 \leq \lambda \leq 2\pi$, $0 \leq \theta \leq \pi$), $d\sigma = \sin\theta d\lambda d\theta$, and where, for $n \geq 0$,

$$\bar{Y}_{nm}(\theta, \lambda) = \bar{P}_{n|m|}(\cos\theta) \begin{cases} \cos m\lambda, & m \geq 0 \\ \sin |m|\lambda, & m < 0 \end{cases} \quad (2)$$

These are the (surface) spherical harmonic functions, which satisfy the following orthogonality property:

$$\frac{1}{4\pi} \iint_{\sigma} \bar{Y}_{nm}(\theta, \lambda) \bar{Y}_{\ell k}(\theta, \lambda) d\sigma = \begin{cases} 1 & \text{if } n = \ell \text{ and } m = k \\ 0 & \text{if } n \neq \ell \text{ or } m \neq k \end{cases} \quad (3)$$

In the mathematical literature the \bar{Y}_{nm} are sometimes defined using the exponential of a complex angle; however, the use of the sinusoidal functions as in (2) is more common in physical geodesy. The \bar{P}_{nm} are the fully normalized associated Legendre functions:

$$P_{nm}(\cos\theta) = \sqrt{\frac{(2n+1)(n-m)!}{\epsilon_m (n+m)!}} P_{nm}(\cos\theta) \quad (4)$$

where $\epsilon_0 = 1$, $\epsilon_m = \frac{1}{2}$, $m \neq 0$, and where $P_{nm}(\cos\theta) = \sin^m\theta \cdot \frac{d^m}{d(\cos\theta)^m} P_n(\cos\theta)$, and the P_n are the well known Legendre polynomials. The set of coefficients $\{f_{nm}\}$, by definition, constitutes the (spherical Legendre) spectrum of F . As noted in the introduction, a different spectrum can be defined by replacing (not a formal change of variable) the geocentric colatitude by the complement of either the geodetic latitude or the reduced latitude. Since any function defined on the sphere is intrinsically periodic in both variables θ and λ , the spectrum is a discrete (but generally infinite) set of numbers (see Papoulis, 1976, p.70).

The inverse Legendre transform is then defined as

$$L_2^{-1}[f_{nm}] = \sum_{n=0}^{\infty} \sum_{m=-n}^n f_{nm} \bar{Y}_{nm}(\theta, \lambda) = F(\theta, \lambda) \quad (5)$$

The last equality follows only if F is continuous, but the series converges under less stringent conditions (Hobson, 1965, p.342). Equations (1) and (5) express a duality between a function and its spectrum. Given the function, its spectrum is unique; and conversely, a given spectrum determines the function uniquely as long as the series (5) converges. Definitions (1) and (5) differ from those of Robertson (1978), but the symmetry of the above transforms is too strong to resist. Unfortunately, this requires some sacrifice in symmetry for the one-dimensional Legendre transform and its inverse ($m=0$ in (1) and (5)):

$$L_1[F] = \frac{\sqrt{2n+1}}{2} \int_0^\pi F(\theta) P_n(\cos\theta) \sin\theta d\theta = f_n \quad (6)$$

$$L_2^{-1}[f_n] = \sum_{n=0}^{\infty} \sqrt{2n+1} f_n P_n(\cos\theta) = F(\theta) \quad (7)$$

The coefficients $\{f_n\}$ constitute the spectrum of F when the basis functions are the zero-order fully normalized associated Legendre functions. Since a one-dimensional function defined on a circle is more conveniently transformed using the Fourier transform, the one-dimensional Legendre transform, per se, will not be considered further. Any function depending only on θ is to be regarded here as a function defined on the sphere and independent of λ ; thus if $\partial F/\partial\lambda = 0$, then $F(\theta) \equiv F(\theta, \lambda)$. Its spectrum, as given by (1), is $\{f_{n0}\} \equiv \{f_n\}$.

The spectrum of a function defined on a sphere depends on the orientation of the coordinate system. Consider the rotation of the coordinate system by the Euler angles α , β , γ (see Fig. 1). Diverting momentarily to Cartesian coordinates x, y, z , the spherical harmonics are homogeneous polynomials (Kellogg, 1953, p.139), which under linear transformations, such as rotations, transform into homogeneous polynomials of the same degree. The maximal set of independent spherical harmonics of degree n comprises the $2n+1$ harmonics of degree n and orders k , $k=-n, \dots, n$. Hence the transformed spherical harmonic $\bar{Y}_{nm}(\psi, \xi)$ in the new coordinate system can be expressed as a linear combination of the harmonics $\bar{Y}_{nk}(\theta, \lambda)$, $k=-n, \dots, n$:

$$\bar{Y}_{nm}(\psi, \xi) = \sum_{k=-n}^n C_{nkm}(\alpha, \beta, \gamma) \bar{Y}_{nk}(\theta, \lambda) \quad (8)$$

where the C_{nkm} are coefficients depending on the Euler angles (see also Müller, 1966; and Kaula, 1959). Cushing (1975, p.596) gives the transformation coefficients explicitly, but for spherical harmonics defined with the exponential of complex multiples of the longitude. Adapting this result to the definition of the spherical harmonics as given by (2), it is only a matter of careful manipulation to derive

$$C_{nkm} = \begin{cases} \frac{(-1)^m}{\sqrt{2\epsilon_m}} [(-1)^k c_{km}^n + c_{-km}^n], & k > 0, m \geq 0 \\ \frac{(-1)^m}{\sqrt{\epsilon_m}} c_{0m}^n, & k = 0, m \geq 0 \\ \frac{(-1)^m}{\sqrt{2\epsilon_m}} [(-1)^k s_{-km}^n - s_{km}^n], & k < 0, m \geq 0 \\ (-1)^k s_{km}^n + s_{-km}^n, & k > 0, m < 0 \\ \sqrt{2} s_{0m}^n, & k = 0, m < 0 \\ -(-1)^k c_{-km}^n + c_{km}^n, & k < 0, m < 0 \end{cases} \quad (9)$$

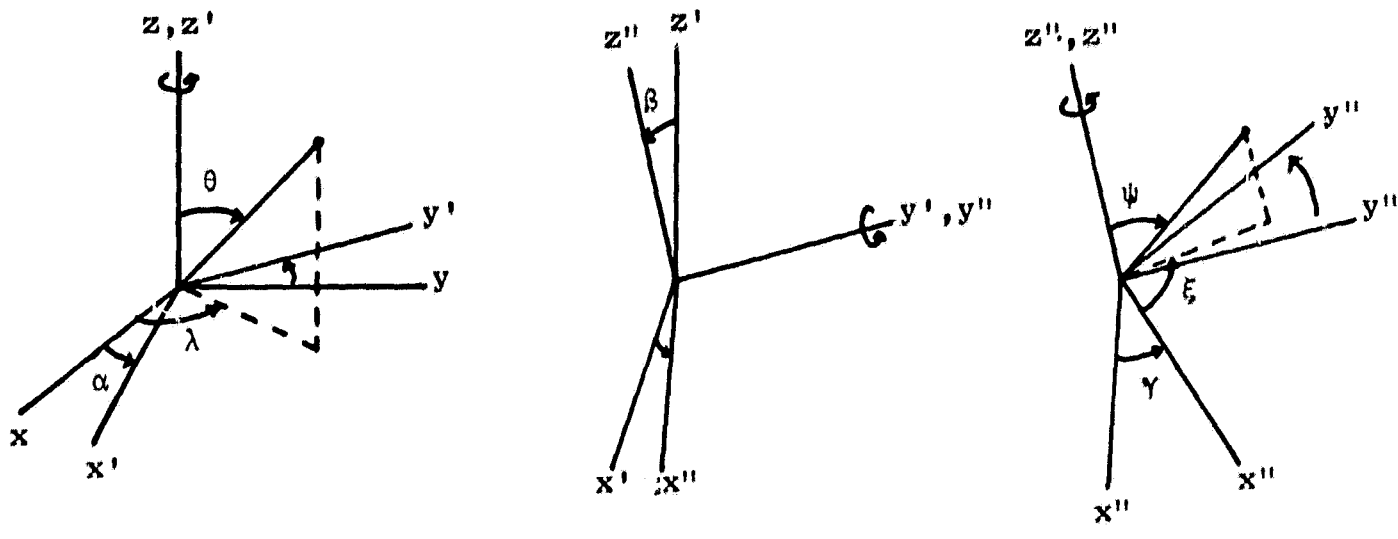


Figure 1: Euler angles α , β , γ

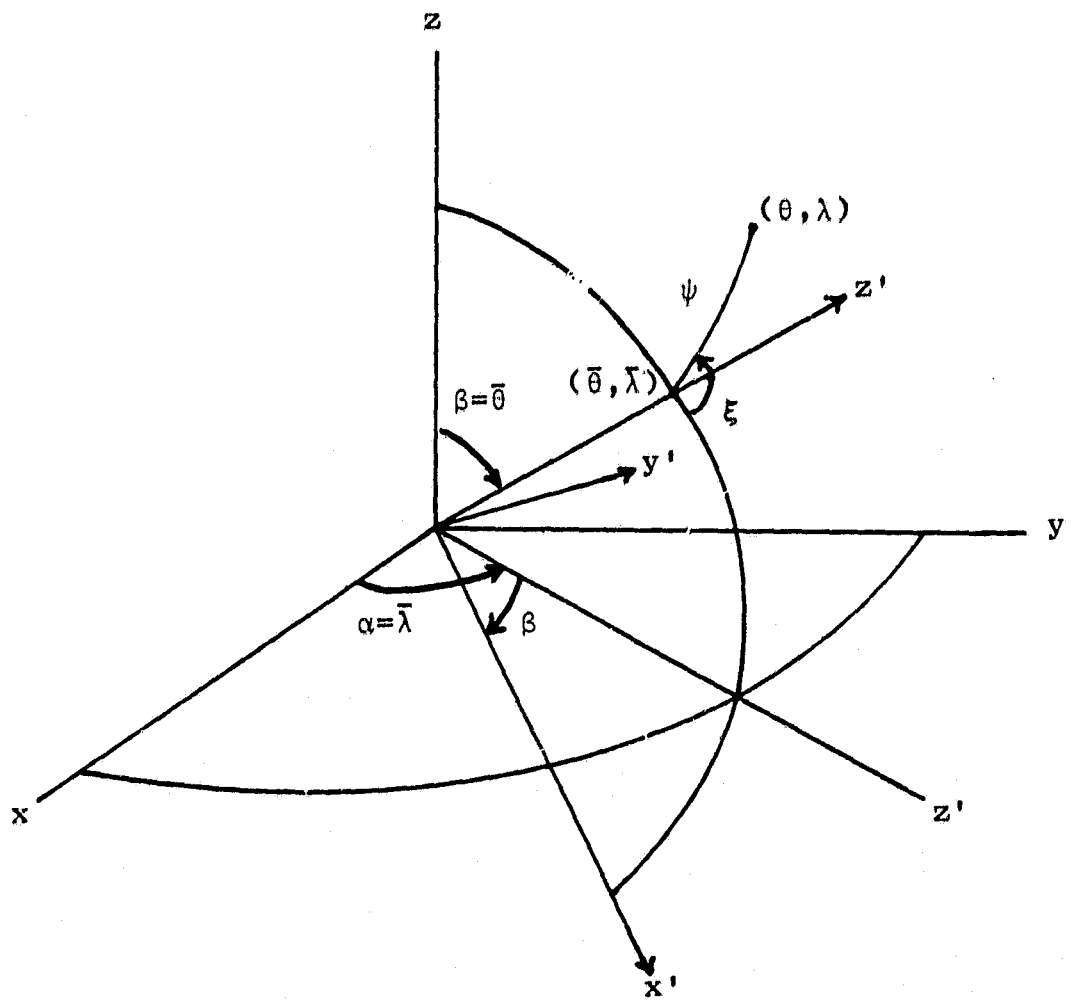


Figure 2: Coordinate Systems θ , λ and ψ , ξ ($\gamma = 0$)

where

$$c_{km}^n = \cos(k\alpha + m\gamma) d_{km}^n(\beta)$$

$$s_{km}^n = \sin(k\alpha + m\gamma) d_{km}^n(\beta) \quad (10)$$

and

$$d_{km}^n(\beta) = (-1)^{k-m} 2^m \sqrt{\frac{(n+m)!(n-m)!}{(n+k)!(n-k)!}} (1 + \cos\beta)^{\frac{-k-m}{2}} (1 - \cos\beta)^{\frac{k-m}{2}} \cdot \frac{1}{2^{n+m}} \sum_{\ell=0}^{n+m} \binom{n+k}{\ell} \binom{n-k}{n+m-\ell} (-1)^{n+m-\ell} (1 - \cos\beta)^{\ell+m-\ell} (1 + \cos\beta)^{\ell}$$

The sum in (11) including the antecedent power of 2 is the Jacobi polynomial $P_{n+m}^{(k-m, -k-m)}(\cos\beta)$. Note that both integers k and m can assume positive as well as negative values and they must be taken literally in the context of each of the foregoing expressions (e.g. if $k, m < 0$, then $-k, -m$ are positive, and the argument of $\sin(k\alpha + m\gamma)$ is negative, etc.). Finally, we note that the binomial coefficients in the expression for the Jacobi polynomial are defined such that $\binom{p}{q} = 0$, if $q > p$, so that the summation extends only over those indices ℓ for which

$$\max(0, m+k) \leq \ell \leq \min(n+k, n+m) \quad (12)$$

for any k, m . If $\gamma = 0$, then

$$C_{nkm} = \begin{cases} (-1)^m \frac{1}{\sqrt{2\epsilon_m}} \cos k\alpha [(-1)^k d_{km}^n(\beta) + d_{-km}^n(\beta)], & k > 0, m \geq 0 \\ \frac{(-1)^m}{\sqrt{\epsilon_m}} d_{0m}^n(\beta), & k = 0, m \geq 0 \\ (-1)^m \frac{1}{\sqrt{2\epsilon_m}} \sin |k|\alpha [(-1)^k d_{-km}^n(\beta) + d_{km}^n(\beta)], & k < 0, m \geq 0 \\ \sin k\alpha [(-1)^k d_{km}^n(\beta) - d_{-km}^n(\beta)], & k > 0, m < 0 \\ 0, & k = 0, m < 0 \\ \cos k\alpha [-(-1)^k d_{-km}^n(\beta) + d_{km}^n(\beta)], & k < 0, m < 0 \end{cases} \quad (13)$$

And if $\alpha = \bar{\lambda}$, $\beta = \bar{\theta}$, $\gamma = 0$, $m = 0$ (see Figure 2), then we obtain the familiar addition theorem for Legendre polynomials:

$$P_n(\cos\psi) = \frac{1}{2n+1} \sum_{m=-n}^n \bar{Y}_{nm}(\bar{\theta}, \bar{\lambda}) Y_{nm}(\theta, \lambda) \quad (14)$$

where $\cos\psi = \cos\theta \cos\bar{\theta} + \sin\theta \sin\bar{\theta} \cos(\lambda - \bar{\lambda})$.

An important concept in signal and time series analysis, arising also frequently in geodesy, is the concept of convolution. For example, the Stokes function convolved with the gravity anomaly results in the geoid undulation (see Robertson (1978) for other examples). The convolution of two one-dimensional functions F , G defined on the real line is formulated as

$$H(\bar{x}) = (G * F)(\bar{x}) = \int_{-\infty}^{\infty} G(\bar{x} - x) F(x) dx \quad (15)$$

The convolution theorem in Fourier analysis is well known (Bath, 1974, p.79); it states that (aside from a constant factor) the (Fourier) spectrum of the convolution H is the product of the (Fourier) spectra of F and G . The process of convolution in the space domain is thus transformed into the computationally simpler process of multiplication in the frequency domain. A similar result holds for convolutions on a sphere.

Churchill and Dolph (1954) defined the convolution of two one-dimensional functions whose spectra are given by the Legendre transform. Since functions depending only on θ here are to be regarded as two-dimensional functions on the unit sphere, but independent of λ , the following definition of convolution differs from theirs:

$$H(\bar{\theta}) = (G * F)(\bar{\theta}) = \frac{1}{4\pi} \int_0^{2\pi} \int_0^{\pi} G(\psi) F(\theta) \sin\theta d\theta d\psi \quad (16)$$

where $\cos\psi = \cos\theta \cos\bar{\theta} + \sin\theta \sin\bar{\theta} \cos\nu$. The variable ν is part of the definition of the convolution and is necessary to derive a corresponding convolution theorem. Let $\{f_n\}$, $\{g_n\}$ be the (Legendre) spectra of F and G , respectively. Then with the addition theorem (14) we have

$$\begin{aligned} G(\psi) &= \sum_{n=0}^{\infty} g_n P_n(\cos\psi) \\ &= \sum_{n=0}^{\infty} \frac{g_n}{\sqrt{2n+1}} \sum_{m=-n}^n \bar{Y}_{nm}(\theta, \nu + \bar{\lambda}) Y_{nm}(\bar{\theta}, \bar{\lambda}) \end{aligned} \quad (17)$$

for arbitrary $\bar{\lambda}$. In this and all following derivations the uniform convergence of the inverse transforms is presumed, so that the summation and integration may be freely interchanged. Therefore

$$H(\bar{\theta}) = \sum_{n=0}^{\infty} \frac{g_n}{\sqrt{2n+1}} \sum_{m=-n}^n \bar{Y}_{nm}(\bar{\theta}, \bar{\lambda})$$

$$\frac{1}{4\pi} \int_{\nu=0}^{2\pi} \int_{\theta=0}^{\pi} \bar{Y}_{nm}(\theta, \nu + \bar{\lambda}) F(\theta) \sin\theta \, d\theta \, d\nu \quad (18)$$

Substituting (2), the integral on the right side is zero unless $m=0$; hence with (6)

$$H(\bar{\theta}) = \sum_{n=0}^{\infty} \frac{g_n f_n}{\sqrt{2n+1}} \bar{P}_{n0}(\cos\bar{\theta}) \quad (19)$$

The (Legendre) spectrum of H is therefore $\frac{1}{\sqrt{2n+1}} f_n g_n$, not exactly the product of the spectra of F and G as in the case of the Fourier transforms.

The convolution of a longitude-independent function G with a function F of both variables may be defined as

$$H(\bar{\theta}, \bar{\lambda}) = (G * F)(\bar{\theta}, \bar{\lambda}) = \frac{1}{4\pi} \int_0^{2\pi} \int_0^{\pi} G(\psi) F(\theta, \lambda) \sin\theta \, d\theta \, d\theta \quad (20)$$

where in this case

$$\cos\psi = \cos\theta \cos\bar{\theta} + \sin\theta \sin\bar{\theta} \cos(\lambda - \bar{\lambda}) \quad (21)$$

The corresponding convolution theorem is established by substituting (17) with $\nu = \lambda - \bar{\lambda}$ into (20):

$$H(\bar{\theta}, \bar{\lambda}) = \sum_{n=0}^{\infty} \frac{g_n}{\sqrt{2n+1}} \sum_{m=-n}^n \bar{Y}_{nm}(\bar{\theta}, \bar{\lambda}) \frac{1}{4\pi} \iint_{\sigma} F(\theta, \lambda) \bar{Y}_{nm}(\theta, \lambda) \, d\sigma$$

$$= \sum_{n=0}^{\infty} \sum_{m=-n}^n \frac{g_n f_{nm}}{\sqrt{2n+1}} \bar{Y}_{nm}(\bar{\theta}, \bar{\lambda}) \quad (22)$$

where (1) was used. The spectrum of H is therefore

$$h_{nm} = \frac{1}{\sqrt{2n+1}} g_n f_{nm} \quad (23)$$

A result differing considerably from the one-dimensional Fourier analogue. The analogy is almost completely lost because the spectrum of G is actually the set $\{g_{nm}\}$, which consists only of zonal coefficients, i.e. $g_{n0} = g_n$ and $g_{nm} = 0$, if $m \neq 0$.

In the area of functional analysis, the convolution integral (20) is viewed as an operator,

$$\Gamma \equiv \frac{1}{4\pi} \iint_{\sigma} G(\psi) (\cdot) d\sigma \quad (24)$$

with an associated kernel G . Thus $\Gamma F = H$. If the result of operating on a function is a scaled version of the function itself, then it is known as an eigenfunction; the scale factor is called the eigenvalue:

$$\Gamma F = fF \quad (25)$$

Recognizing the set $\{y_{ij} = 1$ if $i = n$ and $j = m$; $y_{ij} = 0$ if $i \neq n$ or $j \neq m\}$ as the spectrum of the spherical harmonic function \bar{Y}_{nm} , the spectrum of the convolution $\Gamma \bar{Y}_{nm}$ is (using (23))

$$\frac{1}{\sqrt{2i+1}} g_i y_{ij} = \begin{cases} \frac{1}{\sqrt{2n+1}} g_n & , \quad \text{if } i = n \text{ and } j = m \\ 0 & , \quad \text{if } i \neq n \text{ or } j \neq m \end{cases} \quad (26)$$

(26) is the spectrum of the function $\frac{1}{\sqrt{2n+1}} g_n \bar{Y}_{nm}$, so that

$$\Gamma \bar{Y}_{nm} = \frac{1}{\sqrt{2n+1}} g_n \bar{Y}_{nm} \quad (27)$$

Therefore, from this slightly different perspective, the eigenfunctions and corresponding eigenvalues of the operator (24) are respectively the spherical harmonic functions $\bar{Y}_{nm}(\theta, \lambda)$ and coefficients $g_n / \sqrt{2n+1}$ (cf. Meissl, 1971).

Finally, a similar definition holds for the convolution of two functions defined on the sphere, each depending on two variables:

$$H(\bar{\theta}, \bar{\lambda}) = (G * F)(\bar{\theta}, \bar{\lambda}) = \frac{1}{4\pi} \iint_{\sigma} G(\psi, \xi) F(\theta, \lambda) d\sigma \quad (28)$$

where ψ , ξ are spherical coordinates, colatitude and longitude, in a system rotated by the angles $\bar{\theta}$, $\bar{\lambda}$; see Fig. 2. A comparatively simple relationship among the spectra of two functions $F(\theta, \lambda)$ and $G(\theta, \lambda)$ and their convolution (equations (28)) does not exist. If we substitute the transformation (8) with the Euler angles $\alpha = \bar{\lambda}$, $\beta = \bar{\theta}$, $\gamma = 0$ into the spectral representation of G , then (28) becomes

$$\begin{aligned} H(\bar{\theta}, \bar{\lambda}) &= \frac{1}{4\pi} \iint_{\sigma} \sum_{n=0}^{\infty} \sum_{m=-n}^n g_{nm} Y_{nm}(\psi, \xi) F(\theta, \lambda) d\sigma \\ &= \sum_{n=0}^{\infty} \sum_{m=-n}^n g_{nm} \sum_{k=-n}^n C_{nkm}(\bar{\theta}, \bar{\lambda}) \frac{1}{4\pi} \iint_{\sigma} F(\theta, \lambda) Y_{nk}(\theta, \lambda) d\sigma \\ &= \sum_{n=0}^{\infty} \sum_{m=-n}^n \sum_{k=-n}^n g_{nm} f_{nk} C_{nkm}(\bar{\theta}, \bar{\lambda}) \end{aligned} \quad (29)$$

The following is a formal derivation of the equation for the spectrum of H , excludes a practical method of computing it, and can be omitted without loss of continuation. The final result is given by equations (37) through (41). Considering (13), we may write

$$C_{nkm}(\bar{\theta}, \bar{\lambda}) = \delta_{km}^n(\bar{\theta}) \begin{cases} \cos k\bar{\lambda} & , k \geq 0 \text{ and } m \geq 0; \text{ or, } k < 0 \text{ and } m < 0 \\ \sin |k|\bar{\lambda} & , k < 0 \text{ and } m \geq 0; \text{ or, } k \geq 0 \text{ and } m < 0 \end{cases} \quad (30)$$

where the definition of $\delta_{km}^n(\bar{\theta})$ can be inferred from (13). We note here only that, according as $k+m$ is either even or odd, $\delta_{km}^n(\bar{\theta})$ is an n -th degree polynomial in $\cos \bar{\theta}$ or $\sin \bar{\theta}$ times a similar polynomial of degree $n-1$. This is verified by noting that the expression for $d_{km}^n(\bar{\theta})$ (equation (11), $\beta = \bar{\theta}$) contains only factors of the form $(1 - \cos \bar{\theta})^{n-p}$, $(1 + \cos \bar{\theta})^p$ ($m+k$ even), or $\sin \bar{\theta} (1 - \cos \bar{\theta})^{n-p-\frac{1}{2}} (1 + \cos \bar{\theta})^{p-\frac{1}{2}}$ ($m+k$ odd), where $p = \frac{1}{2}(k+m) \geq 0$ (always). The $C_{nkm}(\bar{\theta}, \bar{\lambda})$ are therefore analytic functions and can be expanded as series of spherical harmonics:

$$C_{nkm}(\bar{\theta}, \bar{\lambda}) = \sum_{i=0}^{\infty} \sum_{j=-i}^i \tau_{ijnm} Y_{ij}(\bar{\theta}, \bar{\lambda}) \quad (31)$$

By (1) and (5)

$$\tau_{ijnm} = \frac{1}{4\pi} \iint_{\sigma} \delta_{km}^n(\bar{\theta}) \begin{pmatrix} \cos k\bar{\lambda} \\ \sin |k|\bar{\lambda} \end{pmatrix} P_{i|j|}(\cos \bar{\theta}) \begin{pmatrix} \cos j\bar{\lambda} \\ \sin |j|\bar{\lambda} \end{pmatrix} d\sigma \quad (32)$$

Invoking the orthogonality of the sinusoids, we have

$$\zeta_{ijnm} = \begin{cases} 0 & ; j \neq k(m \geq 0), j \neq -k(m < 0) \\ \frac{\epsilon_k}{2} \int_0^\pi \delta_{km}^n(\bar{\theta}) P_{i|k|}(\cos \bar{\theta}) \sin \bar{\theta} d\bar{\theta} & ; j = k(m \geq 0), j = -k(m < 0) \end{cases} \quad (33)$$

Hence, because i cannot be less than $|k|$, (31) becomes

$$C_{nkm}(\bar{\theta}, \bar{\lambda}) = \sum_{i=|k|}^{\infty} \zeta_{ik*nm} \bar{Y}_{ik*}(\bar{\theta}, \bar{\lambda}) \quad (34)$$

where $k* = (\text{sign of } m) \cdot k$. Substituting this into (29) yields

$$H(\bar{\theta}, \bar{\lambda}) = \sum_{n=0}^{\infty} \sum_{m=-n}^n \sum_{k=-n}^n \sum_{i=|k|}^{\infty} g_{nm} f_{nk} \zeta_{ik*nm} \bar{Y}_{ik*}(\bar{\theta}, \bar{\lambda}) \quad (35)$$

Now it is easily recognized that, symbolically, $\sum_{n=0}^{\infty} \sum_{m=-n}^n = \sum_{m=-\infty}^{\infty} \sum_{n=|m|}^{\infty}$; therefore, by first transposing summation signs, we have

$$\begin{aligned} \sum_{n=0}^{\infty} \sum_{m=-n}^n \sum_{k=-n}^n \sum_{i=|k|}^{\infty} &= \sum_{n=0}^{\infty} \sum_{k=-n}^n \sum_{i=|k|}^{\infty} \sum_{m=-n}^n \\ &= \sum_{k=-\infty}^{\infty} \sum_{n=|k|}^{\infty} \sum_{i=|k|}^{\infty} \sum_{m=-n}^n \\ &= \sum_{i=0}^{\infty} \sum_{k=-i}^i \sum_{n=|k|}^{\infty} \sum_{m=-n}^n \end{aligned} \quad (36)$$

It can then be verified that

$$H(\bar{\theta}, \bar{\lambda}) = \sum_{i=0}^{\infty} \sum_{k=-i}^i \sum_{n=|k|}^{\infty} \sum_{m=-n}^n \chi_{iknm} \bar{Y}_{ik}(\bar{\theta}, \bar{\lambda}) \quad (37)$$

where

$$\chi_{iknm} = \begin{cases} g_{nm} f_{nk} \zeta_{iknm}, & m \geq 0 \\ g_{nm} f_{n,-k} \zeta_{iknm}, & m < 0 \end{cases} \quad (38)$$

and

$$\zeta_{iknm} = \frac{\epsilon k}{2} \int_0^\pi \delta_{km}^n(\bar{\theta}) \bar{P}_{i|k|}(\cos\bar{\theta}) \sin\bar{\theta} d\bar{\theta} \quad (39)$$

Finally,

$$H(\bar{\theta}, \bar{\lambda}) = \sum_{i=0}^{\infty} \sum_{k=-i}^i h_{ik} Y_{ik}(\bar{\theta}, \bar{\lambda}) \quad (40)$$

where

$$h_{ik} = \sum_{n=|k|}^{\infty} \sum_{m=-n}^n \chi_{iknm} \quad (41)$$

The set $\{h_{ik}\}$ is the spectrum of the convolution (28). The evaluation of h_{ik} , given the spectra of F and G , involves an infinite summation, as well as the computation of the integrals (39).

Clearly, from the above discussions, the powerful convolution theorem of Fourier analysis cannot be adapted blindly to two-dimensional spherical functions. Although the spectrum of the spherical convolution also involves the products of the spectra of the functions being convolved, the relationships are generally not as straight forward as in the Cartesian case.

To conclude this section the Dirac delta function is defined on the unit sphere. In the rectilinear case, this function, denoted $\delta(x)$, is defined to be zero everywhere on the real line except at a single point \bar{x} such that for a continuous function $F(x)$

$$\int_{-\infty}^{\infty} \delta(x - \bar{x}) F(x) dx = F(\bar{x}) \quad (42)$$

The spherical equivalent of $\delta(x)$ is defined similarly, but here we assume that it is also isotropic, i.e. independent of the direction between the point of integration and point where it is nonzero. Denoting it by $D(\psi)$, we have (by definition)

$$\frac{1}{4\pi} \iint_{\sigma} D(\psi) F(\theta, \lambda) d\sigma = F(\bar{\theta}, \bar{\lambda}) \quad (43)$$

where ψ is the spherical distance between (θ, λ) and $(\bar{\theta}, \bar{\lambda})$ (see (21)). The spectrum of $D(\psi)$ is (see (1))

$$d_{nm} = \frac{1}{4\pi} \iint_{\sigma} D(\psi) \bar{Y}_{nm}(\psi, \xi) \sin\psi \, d\psi \, d\xi$$

$$= \begin{cases} 0 & , \quad m \neq 0 \\ \frac{1}{4\pi} \iint_{\sigma} D(\psi) \bar{P}_{n0}(\cos\psi) \, d\sigma & , \quad m = 0 \end{cases} \quad (44)$$

Hence, using (43),

$$d_n = \bar{P}_{n0}(\cos 0^\circ) = \sqrt{2n+1} \quad (45)$$

The operation associated with the delta function is a convolution of the type (20). In the realm of functional analysis in Hilbert space, $D(\psi)$ is an example of a reproducing kernel (see Krarup, 1969, p.43).

3. The Mean Gravity Anomaly

In this section some of the mathematical tools developed above are implemented to study the smoothing of the gravity field. The (point) gravity anomaly, with the standard spherical approximation already applied, has the following series representation (Heiskanen and Moritz, 1967, pp. 89, 108):

$$\Delta g(r, \theta, \lambda) = \gamma \sum_{n=0}^{\infty} (n-1) \left(\frac{R}{r}\right)^{n+2} \sum_{m=0}^n (\bar{C}_{nm} \cos m\lambda + \bar{S}_{nm} \sin m\lambda) \bar{P}_{nm}(\cos\theta) \quad (46)$$

where r is the distance from the center of the earth; $\gamma = kM/R^2$ is an average value of gravity; kM is the product of the gravitational constant and the earth's mass; R is the radius of the sphere that approximates the earth's surface; and \bar{C}_{nm} , \bar{S}_{nm} are constant, dimensionless coefficients. Equation (46) may be rewritten in the more compact form as

$$\Delta g(r, \theta, \lambda) = \sum_{n=0}^{\infty} \sum_{m=-n}^n \left(\frac{R}{r}\right)^{n+2} A_{nm} \bar{Y}_{nm}(\theta, \lambda) \quad (47)$$

where the coefficients,

$$A_{nm} = \begin{cases} \gamma(n-1) \bar{C}_{nm} & , \quad m \geq 0 \\ \gamma(n-1) \bar{S}_{nm} & , \quad m < 0 \end{cases} \quad (48)$$

constitute the spectrum of the gravity anomaly on the sphere of radius R . It is worth noting that the spectrum on a sphere of radius $r=R_1 > R$ is given by the set of coefficients $\{(R/R_1)^{n+2} A_{nm}\}$.

From the introductory remarks, the mean gravity anomaly is derived from the point anomaly by subjecting the latter to an averaging process. Mathematically, we formulate this by applying an operator (only isotropic operators will be considered), such as,

$$\frac{1}{4\pi} \iint_{\Delta\sigma} B(\psi)(\cdot) d\sigma \quad (49)$$

to the gravity anomalies within the region $\Delta\sigma$ on the earth's surface. Because the kernel of this operator, $B(\psi)$, is supposed to depend only on ψ (i.e. the spherical distance between the point of computation and the point of integration), the region is necessarily a spherical cap centered at the point of computation. By defining $B(\psi)=0$ outside the cap we obtain the following more general formulation of the weighted average:

$$\Delta\bar{g}(\bar{\theta}, \bar{\lambda}) = \frac{1}{4\pi} \iint_{\sigma} B(\psi) \Delta g(\theta, \lambda) d\sigma \quad (50)$$

The operator thereby becomes a member of the class of operators (24), and the operation itself is a convolution of the type (20). For convenience, we may write the kernel as a normalized weighting function:

$$B(\psi) = \frac{w(\psi)}{\frac{1}{4\pi} \iint_{\sigma} w(\psi) d\sigma} \quad (51)$$

where $|w(\psi)| \leq 1$ for $0 \leq \psi \leq \pi$. Now let $\{b_n\}$ be its spectrum, i.e.

$$B(\psi) = \sum_{n=0}^{\infty} \sqrt{2n+1} b_n P_n(\cos\psi) \quad (52)$$

where, according to (6) and (7),

$$b_n = \frac{\sqrt{2n+1}}{2} \int_0^{\pi} B(\psi) P_n(\cos\psi) \sin\psi d\psi \quad (53)$$

The convolution theorem, enunciated by equations (22) and (23), then directly provides the spectrum of the mean anomaly

$\bar{\Delta g}$:

$$\begin{aligned}\bar{A}_{nm} &= \frac{b_n}{\sqrt{2n+1}} A_{nm} \\ &= \beta_n A_{nm}\end{aligned}\tag{54}$$

The constants β_n are the eigenvalues of the averaging operator; or in the jargon of spectral theory, the frequency response of the filter. In view of (54), $|100 \beta_n|$ is the percentage of an (n)th-degree harmonic coefficient that is retained in the process of averaging.

Averaging gravity anomalies over a spherical cap is not a typical operation in geodetic practice. Rather, mean anomalies are viewed as averages over spherical blocks (trapezoids) delimited by convenient global or local curvilinear coordinate lines. The average over such blocks is characterized by operators that are nonisotropic (see Pollack, 1973), and the averaging process is then a convolution of the general type (28). The spectrum of such a mean is difficult to obtain in terms of the point anomaly spectrum (see the previous section). Gaposchkin (1980) derived and studied a series expansion of the mean over a trapezoidal block (however, it is not a spectral representation as defined by (5)). Pollack (1973) compared the β_n corresponding to isotropic operators with the degree variances of the above mentioned nonisotropic operators. Recalling (41), it appears uncertain whether a study of these degree variances is indicative of how the spectrum of the anomaly is transformed in the averaging process. When computing mean anomalies from the point anomaly spectrum, the average over a block is frequently approximated by an average over a cap having the area of the block (Rapp, 1977). This approximation degrades with the elongation of the block (e.g. in the polar regions, where the meridional coordinate lines converge). Some further study is indicated here, but is beyond the scope of this paper.

3.1 The Pellinen Mean

The equally weighted average of the gravity anomaly over a spherical cap is defined as the integral of the anomaly over the cap divided by the cap's area. For this simple average (see also Pellinen, 1966), we have, in agreement with (50) and (51),

$$w_P(\psi) = \begin{cases} 1 & , \quad 0 \leq \psi \leq \psi_0 \\ 0 & , \quad \psi_0 < \psi \leq \pi \end{cases}\tag{55}$$

ψ_0 being the radius (generating angle) of the cap. Substituting the resulting kernel,

$$B_p(\psi) = \frac{4\pi}{2\pi \int_0^{\psi_0} \sin\psi \, d\psi} \quad (56)$$

into (53) yields

$$\begin{aligned} b_{p_n} &= \frac{\sqrt{2n+1}}{1 - \cos\psi_0} \int_0^{\psi_0} P_n(\cos\psi) \sin\psi \, d\psi \\ &= \frac{P_{n-1}(\cos\psi_0) - P_{n+1}(\cos\psi_0)}{\sqrt{2n+1} (1 - \cos\psi_0)} \end{aligned} \quad (57)$$

for which Sjöberg (1979) has found the following recursion formula:

$$\begin{aligned} \beta_{p_n} &= \frac{b_{p_n}}{\sqrt{2n+1}} = \frac{2n-1}{n+1} \cos\psi_0 \beta_{p_{n-1}} - \frac{n-2}{n+1} \beta_{p_{n-2}}, \quad n \geq 2 \\ \beta_{p_0} &= 1, \quad \beta_{p_1} = \frac{1}{2}(1 + \cos\psi_0) \end{aligned} \quad (58)$$

Fig. 3 depicts w_p as a function of ψ for $\psi_0 = 0:564$, which corresponds to a cap whose area equals the area of a $1^\circ \times 1^\circ$ block at the equator. The coefficients β_{p_n} are shown in Fig. 4. Here (as in Fig. 5), for the sake of clarity, the values of the smoothing factors β_n (which are discontinuous functions defined only for integer values of n) are traced by smooth curves.

The spectrum of the Pellinen mean has an infinity of components, but the high-degree coefficients are clearly diminished in magnitude and thus suppress the local structure of the anomaly field. The first zero in the Fourier spectrum of the analogous one-dimensional "rectangular" filter occurs at $n = \pi/\psi_0 = 319$ for $\psi_0 = 0:546$ (Bath, 1974, p.218). This formula is not applicable in the spherical case as $\beta_{p_n}(\psi_0 = 0:564)$ is first negative when $n = 389$. The major drawback of this operator, viewed as a "low-pass" filter, is the presence of the large positive and negative "side lobes" in its spectrum. That is, the filter admits, or passes, a considerable part of the upper end of the spectrum, even changing the sign of some of the coefficients. This "reversal of polarity" could transform minima of the point function into (false) maxima of the mean function, and vice versa (Holloway, 1958); see section 4.

3.2 The Gaussian Mean

This and the following weighting function are adaptations of filters commonly found in electrical engineering (Harris, 1978, gives a good summary). The Gaussian mean takes its name from the bell-shaped normal (Gaussian) probability density function that its weighting function resembles for small ψ :

$$w_G(\psi) = e^{-a(1 - \cos \psi)} \quad , \quad a > 0 \quad , \quad 0 \leq \psi \leq \pi \quad (59)$$

$$\approx e^{-\frac{a}{2} \psi^2} \quad , \quad \text{small } \psi$$

The dimensionless parameters "a" (identifiable with the inverse of the second moment σ^2 of the Gaussian distribution) characterizes the smoothing process. Since

$$\frac{1}{4\pi} \iint_{\sigma} w_G(\psi) \, d\sigma = \frac{1}{2a} (1 - e^{-2a}) \quad (60)$$

the kernel becomes

$$B_G(\psi) = \frac{2ae^{-a(1 - \cos \psi)}}{1 - e^{-2a}} \quad (61)$$

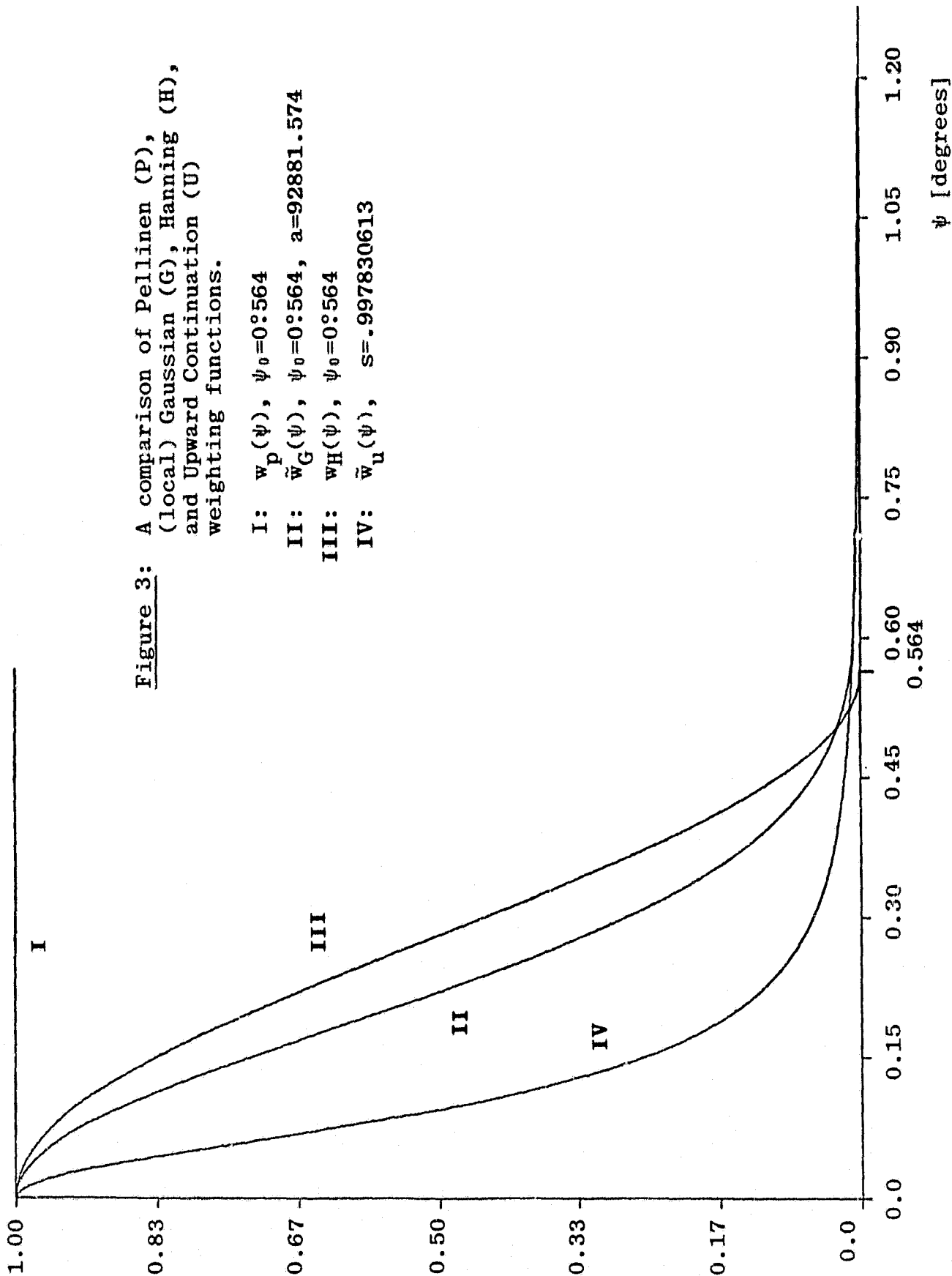
and the eigenvalues of the corresponding operator are

$$\beta_{G_n} = \frac{b_{G_n}}{\sqrt{2n+1}} = \int_{-1}^1 \frac{ae^{-a(1-y)}}{(1 - e^{-2a})} P_n(y) \, dy \quad , \quad y = \cos \psi \quad (62)$$

for which the following recursion formula holds:

$$\begin{aligned} \beta_{G_{n+1}} &= -\frac{2n+1}{a} \beta_{G_n} + \beta_{G_{n-1}} \quad , \quad n \geq 1 \\ \beta_{G_0} &= 1 \quad , \quad \beta_{G_1} = \frac{1 + e^{-2a}}{1 - e^{-2a}} - \frac{1}{a} \end{aligned} \quad (63)$$

(63) is readily verified by applying the relationship $P'_{n+1}(y) = (2n+1)P_n(y) - P'_{n-1}(y)$ in (62) and integrating by parts. The function (59) is a global weighting function to be convolved with gravity anomalies over the entire sphere. On the other hand, restricting the averaging process to a cap,



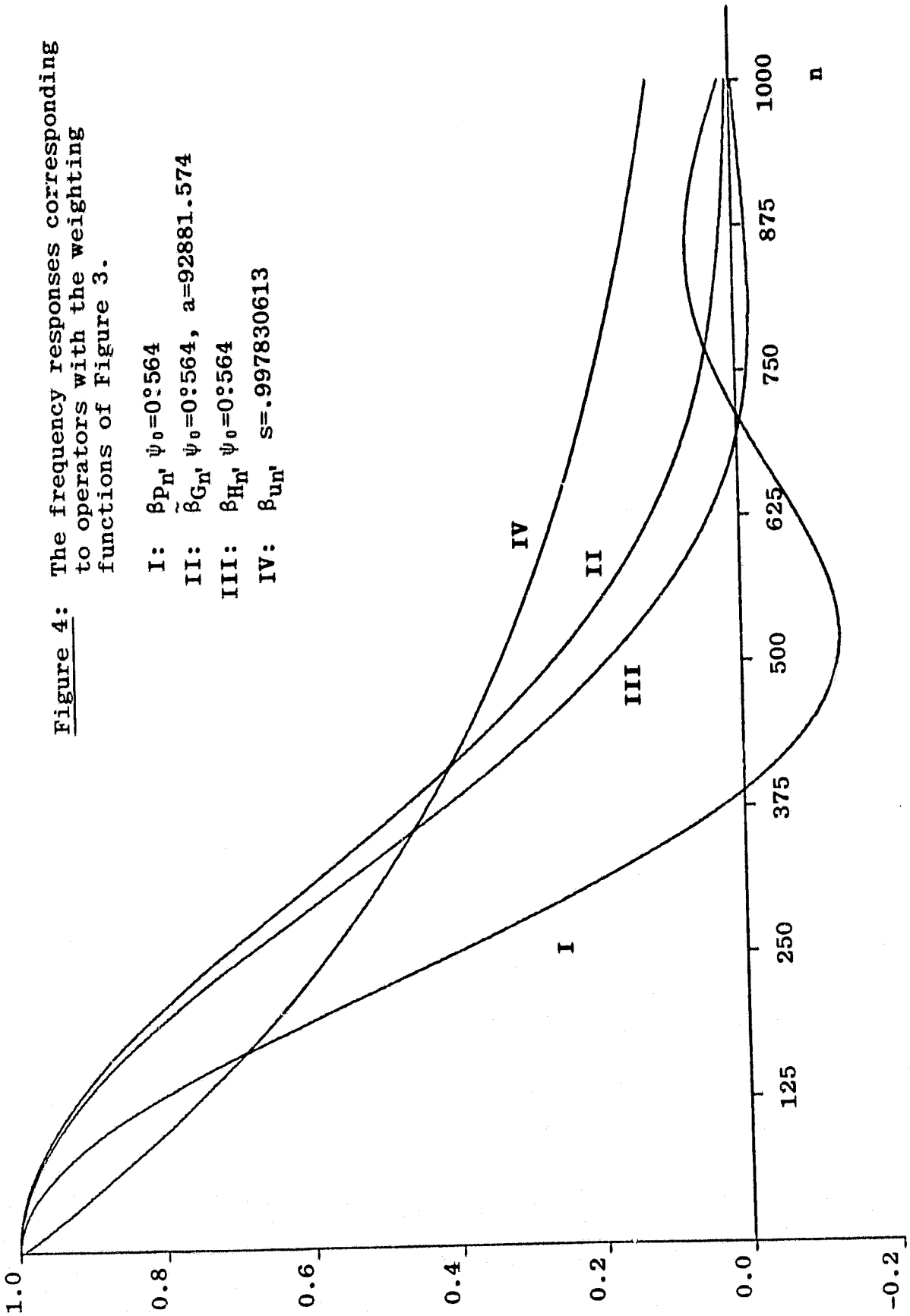


Figure 4: The frequency responses corresponding to operators with the weighting functions of Figure 3.

- I: $\beta_{P_n} \psi_0 = 0.564$
- II: $\tilde{\beta}_{G_n} \psi_0 = 0.564, a = 92881.574$
- III: $\beta_{H_n} \psi_0 = 0.564$
- IV: $\beta_{u_n} s = .997830613$

$\psi_0 = 0.564$, each of the conditions $\tilde{w}_G(\psi_0) = 0.5$, $\tilde{w}_G(\psi_0) = 0.1$, and $3\sigma = \psi_0$ (where $a = 1/\sigma^2$) produces different frequency responses (cases II, III, IV). Also shown (case I) for comparison are the β_{Gn} corresponding to the global weighting function with the condition $w_G(0.564) = 0.5$. The weighting functions associated with these smoothing factors are shown in Fig. 6.

Figures 5 and 6 suggest that as the cap-edge value of the weighting function $\tilde{w}_G(\psi)$ approaches zero (it can never equal zero), the oscillations of the corresponding frequency response decrease in magnitude. Furthermore, the smaller "a" is, the more the higher-degree harmonics are filtered from the anomaly. Designing the Gaussian filter so as to have certain smoothing properties is therefore accomplished by properly choosing values of "a" and ψ_0 . The selection of "a" controls the essential bandwidth of the filter, i.e. what frequencies should be passed; while the subsequent choice of ψ_0 controls the magnitude of the oscillations of the frequency response function. The frequency response of the Gaussian filter defined for data on the real line is given by Holloway (1958, p.359) as

$$g_n = e^{-\frac{1}{2} \frac{n^2}{a}} \quad (70)$$

(where, if f denotes frequency, the relationship $2\pi f = n$ was used). The similarity between β_{Gn} (global filter) and g_n is shown in Table 1 and can be invoked to provide an approximate value of "a" given a desired value of β_{Gn} for some n . For example, if the harmonic at degree \bar{n} is to be suppressed to 100f₀% of its original value (less than 100f₀% of each subsequent harmonic will be passed), then

$$a \approx \frac{\bar{n}^2}{2 \ln(1/f_0)} \quad (71)$$

Table 1: Legendre vs. Fourier Gaussian Frequency Responses

a = 128235			a = 13131		
n	β_{Gn} (equ.(63))	g_n (equ.(70))	n	β_{Gn} (equ.(63))	g_n (equ.(70))
10	.9996	.9996	10	.9958	.9962
50	.9901	.9903	50	.9075	.9092
200	.8549	.8556	75	.8049	.8072
400	.5350	.5359	100	.6807	.6833
600	.2451	.2457	125	.5490	.5516
700	.1476	.1480	150	.4221	.4245
800	.08220	.08246	200	.2164	.2180
900	.04235	.04250	250	.09168	.09256
1000	.02018	.02026	350	.009300	.009424

Figure 5: A comparison of Gaussian frequency responses determined by various constraints on the weighting function.

- I: $a=14306.916, \psi_0=180^\circ$
- II: $\tilde{w}_G(\psi_0)=-.5 (a=14306.915), \psi_0=0:564$
- III: $\tilde{w}_G(\psi_0)=-.1 (a=47526.546), \psi_0=0:564$
- IV: $3\sigma = \psi_0 (a=92881.574), \psi_0=0:564$

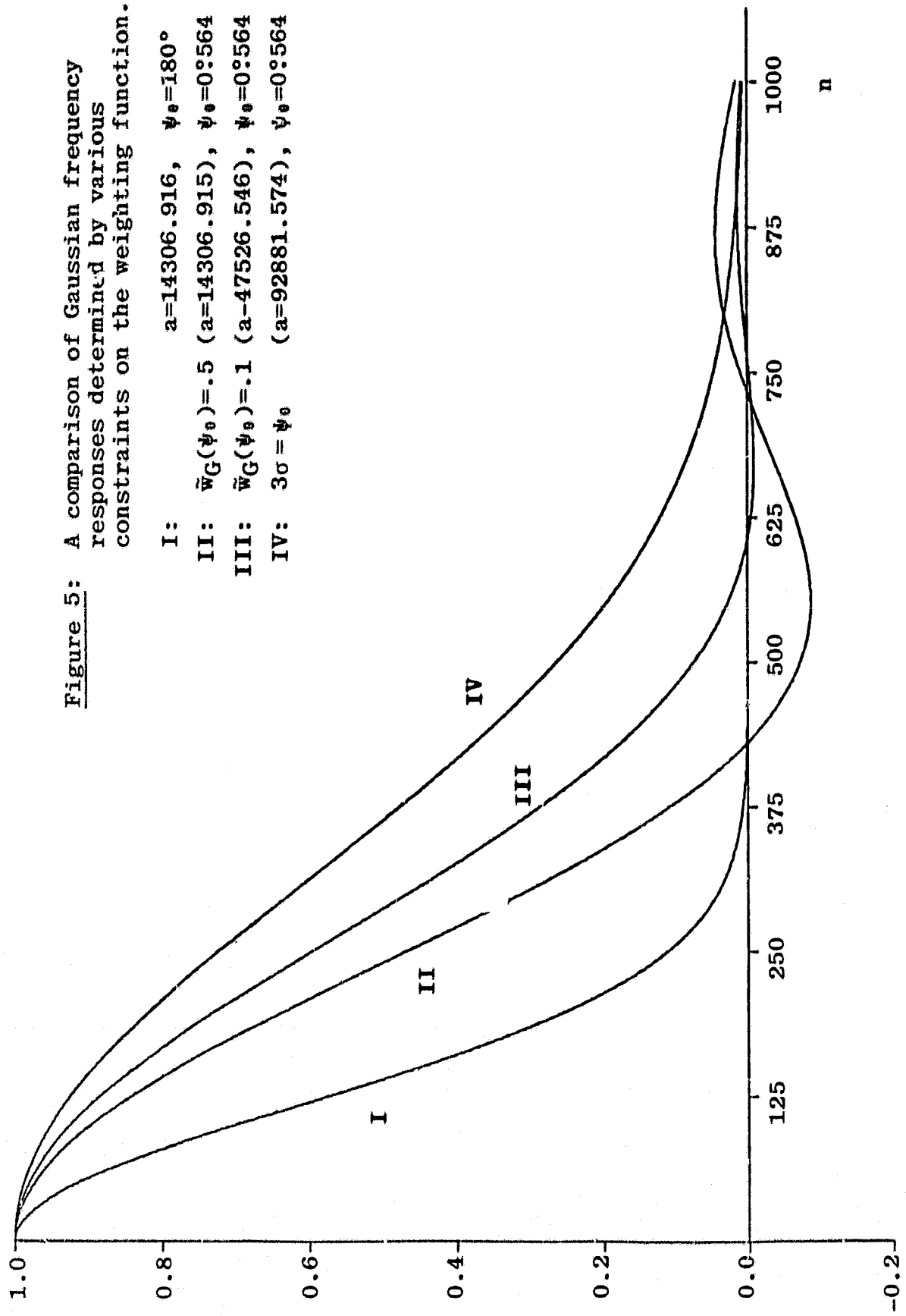
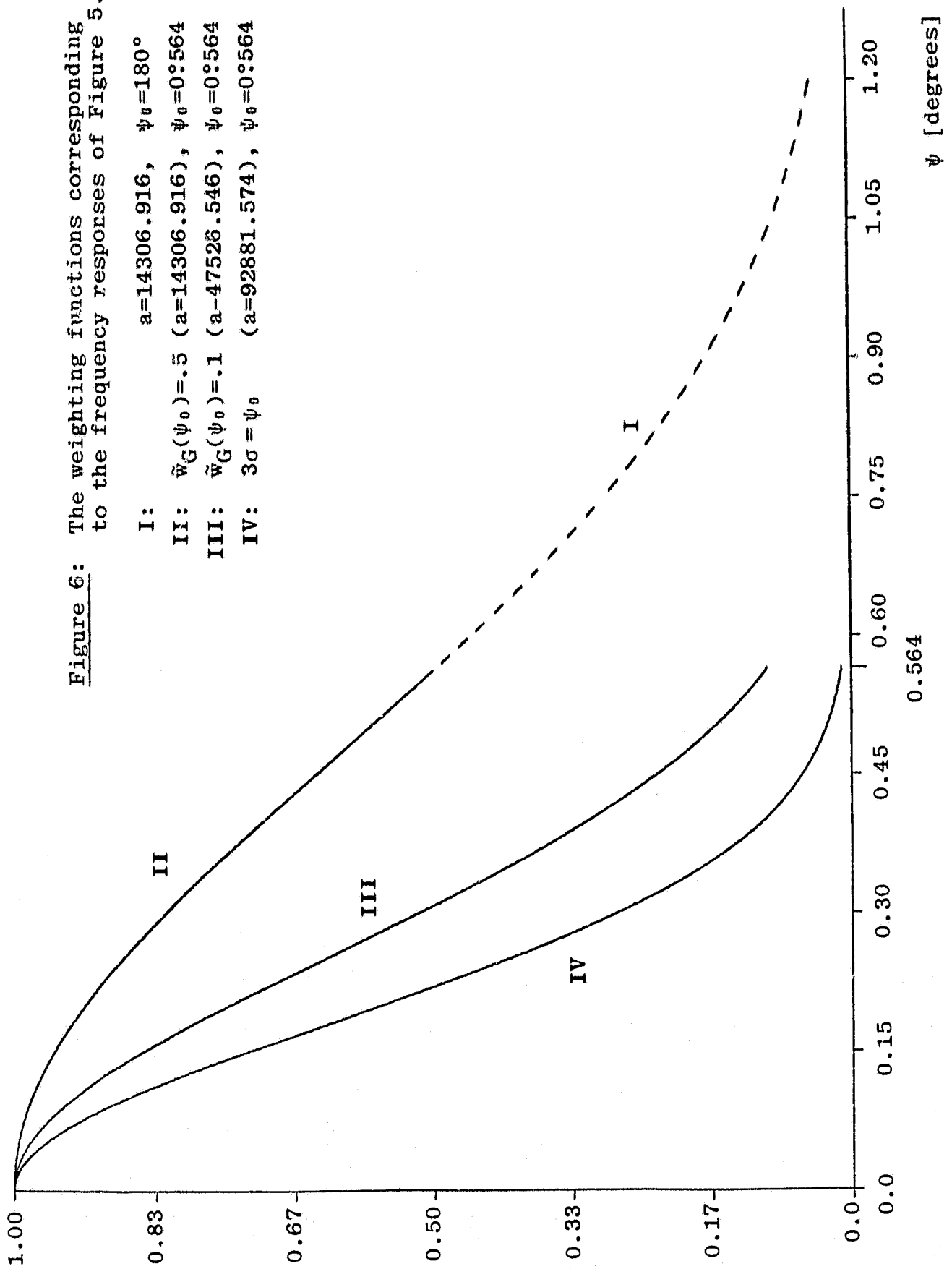


Figure 6: The weighting functions corresponding to the frequency responses of Figure 5.



3.3 The Hanning Mean

The weighting function

$$w_H(\psi) = \begin{cases} \frac{1}{2} \left(1 + \cos \frac{\pi\psi}{\psi_0} \right) , & 0 \leq \psi \leq \psi_0 \\ 0 & , \psi_0 < \psi \leq \pi \end{cases} \quad (72)$$

resembles the Hanning filter whose desirable filtering characteristics (Holloway, 1958; Bath, 1974, p.158) make it popular in the disciplines where it is applicable. (See also (Wenzel and Arabelos (1981) where the Hanning "window function" (72) is used to reduce the integration ("truncation") error incurred when performing an integration of a covariance function over less than the required interval, $0 \leq \psi \leq \pi$. The spectrum of w_H defined by them differs essentially from the definition adopted here, but the spectral properties are similar.)

The eigenvalues of the corresponding Hanning smoothing operator are given by

$$\beta_{H_n} = \frac{\pi^2 - \psi_0^2}{\pi^2(1 - \cos\psi_0) - 2\psi_0^2} \left[\frac{1}{2n+1} (P_{n-1}(\cos\psi_0) - P_{n+1}(\cos\psi_0)) + \alpha_n \right], \quad n \geq 1$$

$$\beta_{H_0} = 1 \quad (73)$$

where

$$\alpha_n = \int_0^{\psi_0} \cos b\psi P_n(\cos\psi) \sin\psi d\psi, \quad b = \frac{\pi}{\psi_0} \quad (74)$$

A recursion formula for α_n ($b \neq \text{integer}$) is derived in Appendix B; it is

$$[(n+1)^2 - b^2] \alpha_n - [(n-2)^2 - b^2] \alpha_{n-2} = (n+1)^2 D_n - (n-2)^2 D_{n-2} + b(E_n - E_{n-2}), \quad n \geq 3 \quad (75)$$

where

$$D_n = \frac{\cos b\psi_0}{2n+1} [P_{n-1}(\cos\psi_0) - P_{n+1}(\cos\psi_0)], \quad n \geq 1$$

$$E_n = \sin b\psi_0 \sin\psi_0 P_n(\cos\psi_0), \quad n \geq 1 \quad (76)$$

and

$$\alpha_0 = \frac{1}{1-b^2} [1 - \cos\psi_0 \cos b\psi_0 - b \sin\psi_0 \sin b\psi_0]$$

$$\alpha_1 = \frac{1}{2(4-b^2)} [2 - 2\cos 2\psi_0 \cos b\psi_0 - b \sin 2\psi_0 \sin b\psi_0] \quad (77)$$

$$\alpha_2 = \frac{3}{8(9-b^2)} [3 - 3\cos 3\psi_0 \cos b\psi_0 - b \sin 3\psi_0 \sin b\psi_0] - \frac{1}{8} \alpha_0$$

The first zero of the Fourier spectrum of the Hanning filter occurs at $n = 2\pi/\psi_0 = 638$, for $\psi_0 = 0^\circ 564$. For the spherical adaptation, $\beta_{Hn}(\psi_0 = 0^\circ 564)$ first changes sign at $n = 695$. Thereafter, the side lobes are comparatively small. Figures 4 and 3 show respectively the frequency response β_{Hn} and the corresponding weighting function w_H .

3.4 The Upward Continuation (Poisson) Operator

Functions harmonic in the space external to a sphere centered at the coordinate origin attenuate radially according to $r^{-(n+1)}$. $r\Delta g$ is such an harmonic function (see equation (46)), and the gravity anomaly field at satellite altitudes, for example, is much smoother than at the earth's surface. Therefore, for a fixed radius, $r = R_1$, the upward continuation operator acts like a smoothing operator with eigenvalues (recall the comment after (48))

$$\beta_{u_n} = \left(\frac{R}{R_1}\right)^{n+2}, \quad n \geq 0 \quad (78)$$

For the disturbing potential the exponent is $n+1$, and for the geoid undulation it is $n-1$; in all cases $\beta_{u_0} \neq 1$, so that, unlike the previous filters, this smoothing process does not leave the global average unaltered (unless $A_{00} = 0$). The corresponding smoothing kernel is

$$\begin{aligned} B_u(\psi) &= \sum_{n=0}^{\infty} (2n+1) \left(\frac{R}{R_1}\right)^{n+2} P_n(\cos\psi), \quad 0 \leq \psi \leq \pi \\ &= \frac{s^2(1-s^2)}{[1-2s\cos\psi+s^2]^{3/2}}, \end{aligned} \quad (79)$$

where $s = R/R_1$ and the familiar generating function for Legendre polynomials was applied. (79) is nothing but s times the kernel of Poisson's integral (Heiskanen and Moritz, 1967, p.35). Because the smoothing is biased (the integral of $4\pi B_u(\psi)$ over the unit sphere is not unity), a weighting function satisfying equation (51) cannot be defined. However, for purposes of comparison, let

$$\tilde{w}_u(\psi) = \frac{B_u(\psi)}{B_u(0)} = \frac{(1-s)^3}{[1-2s\cos\psi+s^2]^{3/2}} \quad (80)$$

Solving for s , we have

$$\begin{aligned} s &= [\tilde{w}_u^{2/3}(\psi) \cos\psi - 1 + (2\tilde{w}_u^{2/3}(\psi)(1-\cos\psi) - \tilde{w}_u^{4/3}(\psi) \sin^2\psi)^{1/2}] \\ &\quad \cdot (\tilde{w}_u^{2/3}(\psi) - 1)^{-1} \end{aligned} \quad (81)$$

Although the entire gravity anomaly field must, in theory, be convolved with the kernel (79) to yield the smoothed field, a specification such as $\tilde{w}_u(\psi_0) = .01$ renders the operation practically a local one. With $\psi = \psi_0 = 0^\circ 564$, equation (81) gives $s = 0.997830613$ (or if $R = 6371000$ m, then $R_1 = 6384851$ m.) \tilde{w}_u and β_{un} with this value of s are shown in Figures 3 and 4.

The upward continuation produces a smoothed field with a more substantial attenuation of the low-degree harmonics, but with a fairly weak taper in the high end of the spectrum. Therefore, it is essentially different from, and less useful for smoothing than, the more conventional (weighted) areal averages.

3.5 The Ideal Filter

Ideally, the smoothing process should suppress the higher-degree harmonics completely with perfect retention of the lower-degree harmonics. This type of smoothing is automatically implemented whenever a determination of the gravity field consists of finding, through satellite techniques, the coefficients of its series representation. Obviously, only a finite number of coefficients can be found and the corresponding truncated series represents a perfectly filtered field (neglecting aliasing and measurement errors). The eigenvalues of the operator that produces such ideal smoothing are

$$\beta_{In} = \begin{cases} 1 & , \quad n = 0, \dots, \bar{n} \\ 0 & , \quad n > \bar{n} \end{cases} \quad (82)$$

where \bar{n} is the desired degree of truncation--the larger \bar{n} is, the less smooth is the filtered field. If the operator is global, the kernel is given by (see (52) and (54))

$$B_I(\psi) = \sum_{n=0}^{\bar{n}} (2n+1) P_n(\cos\psi) \quad (83)$$

(If $\bar{n} \rightarrow \infty$, B_I becomes the spherical equivalent of the Dirac delta function; see (45).)

It is not possible to define a kernel whose convolution with gravity anomalies in a cap with radius $0 < \psi_0 < \pi$ yields a perfectly filtered field. That is, a kernel with a finite spectrum is analytic on the sphere and cannot be zero over any part of the sphere unless it is zero everywhere.

3.6 Discrete Operators

The averaging process in actual practice deals with discrete values of the gravity field--integrations such as (50) are performed numerically often using simple midpoint formulas:

$$\Delta \bar{g}(\bar{\theta}, \bar{\lambda}) = \frac{1}{4\pi} \sum_{j=1}^M B(\psi_j) \Delta g(\theta_j, \lambda_j) \Delta \sigma_j \quad (84)$$

where ψ_j is the geocentric angle between points $(\bar{\theta}, \bar{\lambda})$ and (θ_j, λ_j) , (θ_j, λ_j) is the center point of the area element $\Delta \sigma_j$, and M is the total number of $\Delta \sigma_j$ into which the cap σ_c has been partitioned. The above formula can be rewritten as an integral by utilizing the Dirac delta function $D(\psi)$ (see (43)):

$$\begin{aligned} \Delta \bar{g}(\bar{\theta}, \bar{\lambda}) &= \left(\frac{1}{4\pi}\right)^2 \sum_{j=1}^M B(\psi_j) \iint_{\sigma} D(\hat{\psi}_j) \Delta g(\theta, \lambda) d\sigma \Delta \sigma_j \\ &= \left(\frac{1}{4\pi}\right)^2 \iint_{\sigma} \left(\sum_{j=1}^M B(\psi_j) D(\hat{\psi}_j) \Delta \sigma_j \right) \Delta g(\theta, \lambda) d\sigma \\ &= \left(\frac{1}{4\pi}\right) \iint_{\sigma} \bar{B}(\psi, \xi) \Delta g(\theta, \lambda) d\sigma \end{aligned} \quad (85)$$

where $\cos \hat{\psi}_j = \cos \theta \cos \theta_j + \sin \theta \sin \theta_j \cos(\lambda - \lambda_j)$ and ψ, ξ are the coordinates of the point (θ, λ) in the spherical coordinate system whose pole is the point $(\bar{\theta}, \bar{\lambda})$ (see Fig. 7).

In Fig. 7, (θ_j, λ_j) , $j=1, \dots, M$ are fixed points and as the variable point (θ, λ) moves over the sphere, its position with respect to the point of computation $(\bar{\theta}, \bar{\lambda})$ may be described by the coordinates ψ, ξ , whence the arguments for the kernel \bar{B} . Note that \bar{B} is zero unless (θ, λ) coincides with one of the points (θ_j, λ_j) . Thus the operator is nonisotropic and the convolution is of the type (28). This implies that the frequency response of any of the filters discussed in the previous sections, in practice, is not given by the corresponding β_n . However, if the numerical integration is sufficiently accurate, the general characteristics of the response are retained, as seen in the next section.

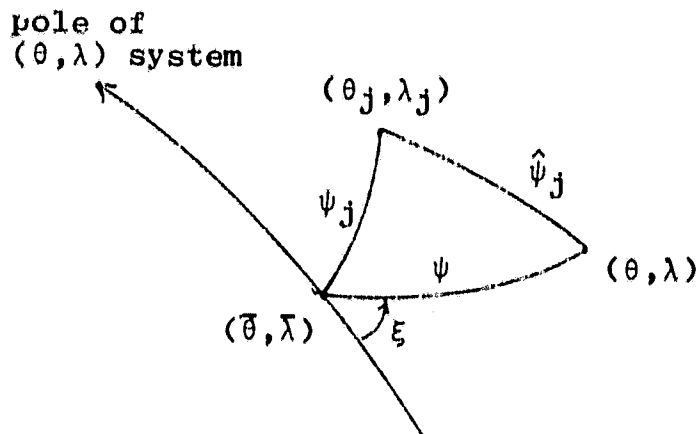


Figure 7: The relationship of (θ, λ) to (θ_j, λ_j) and $(\bar{\theta}, \bar{\lambda})$, equation (85).

4. Smoothing a Simulated Gravity Field

In this section the formulas for the various averaging processes are put into practice, illustrating, by an example, the differences between the Pellinen, Gaussian, and Hanning averages in the space domain. For this purpose, a gravity anomaly field was generated as a series of spherical harmonic functions with coefficients:

$$A_{nm} = \beta_{G_n} \begin{cases} \frac{1}{\beta_{P_n}} [(\text{180,180}) \text{ solution of Rapp (1978)}], & n=2, \dots, 100 \\ u_{nm} \sqrt{\frac{c_n}{d_n}}, & n=101, \dots, 360 \end{cases} \quad (86)$$

where the u_{nm} are random numbers uniformly distributed on the interval $[-0.5, 0.5]$ and d_n is their degree variance. c_n is the degree variance of the gravity anomaly and is modeled (Rapp, 1979) by

$$c_n = 3.405 \frac{n-1}{n+1} (.998006)^{n+2} + 140.03 \frac{n-1}{(n+2)(n-2)} (.914232)^{n+2} \quad [\text{mgal}]^2, n \geq 3 \quad (87)$$

The (180,180) solution was derived from $1^\circ \times 1^\circ$ mean gravity anomalies, and the division by β_{pn} , being the frequency response of the Pellinen averaging operator with $\psi_0 = 0^\circ 564$, effects a relatively smooth transition from the actual (originally mean) spectrum to the modeled (point) spectrum. The smoothing of the coefficients by a Gaussian filter ($a = 14000$, $\psi_0 = \pi$) attenuates the upper spectrum to virtually zero at $n = 360$ ($\beta_{G360} = 0.01$), resulting in a less irregular field for which the differences in the filters are better illustrated.

The gravity anomaly function defined by (86) was evaluated on two profiles near the equator*: $\phi = \pm 1^\circ 5$, $0^\circ 5 \leq \lambda \leq 42^\circ 5$ (see Figures 10 and 11). This function was convolved with the Pellinen smoothing kernel ($\psi_0 = 1^\circ 692$, corresponding to a cap having the area of a $3^\circ \times 3^\circ$ block at the equator), the Gaussian kernel ($\psi_0 = 2^\circ 459$, $a = 4887.27$), and the Hanning kernel ($\psi_0 = 2^\circ 459$). These latter choices for the cap radius and the parameter "a" yield frequency responses that pass generally the same band of frequencies as the Pellinen average; see Figure 8. The precise value of the cap radius was established by requiring the cap to have the area of a finite number of 0.5×0.5 blocks arranged roughly in the shape of a disk, as in Figure 9. The parameter "a" then follows from the stipulated relationship $3\sigma = \psi_0$ ($\sigma^2 = 1/a$).

The mean gravity anomaly function, computed using the smoothed coefficients $\beta_n A_{nm}$, are plotted in Figures 10 and 11 (Pellinen vs. Gaussian averages) and Figures 12 and 13 (Pellinen vs. Hanning averages). The essential feature of these comparison is the 180° phase shift of the Pellinen average with respect to the point function at a wavelength of about 2° , as predicted by the frequency response β_{pn} (in Figure 8, β_{pn} has a maximum negative value at $n = 172$, corresponding to a wavelength of about $360/n = 2^\circ 1$). The Gaussian and Hanning mean functions, on the other hand, reproduce more faithfully the peaks and valleys of the point function, as the corresponding frequency responses have either small or insignificant negative values.

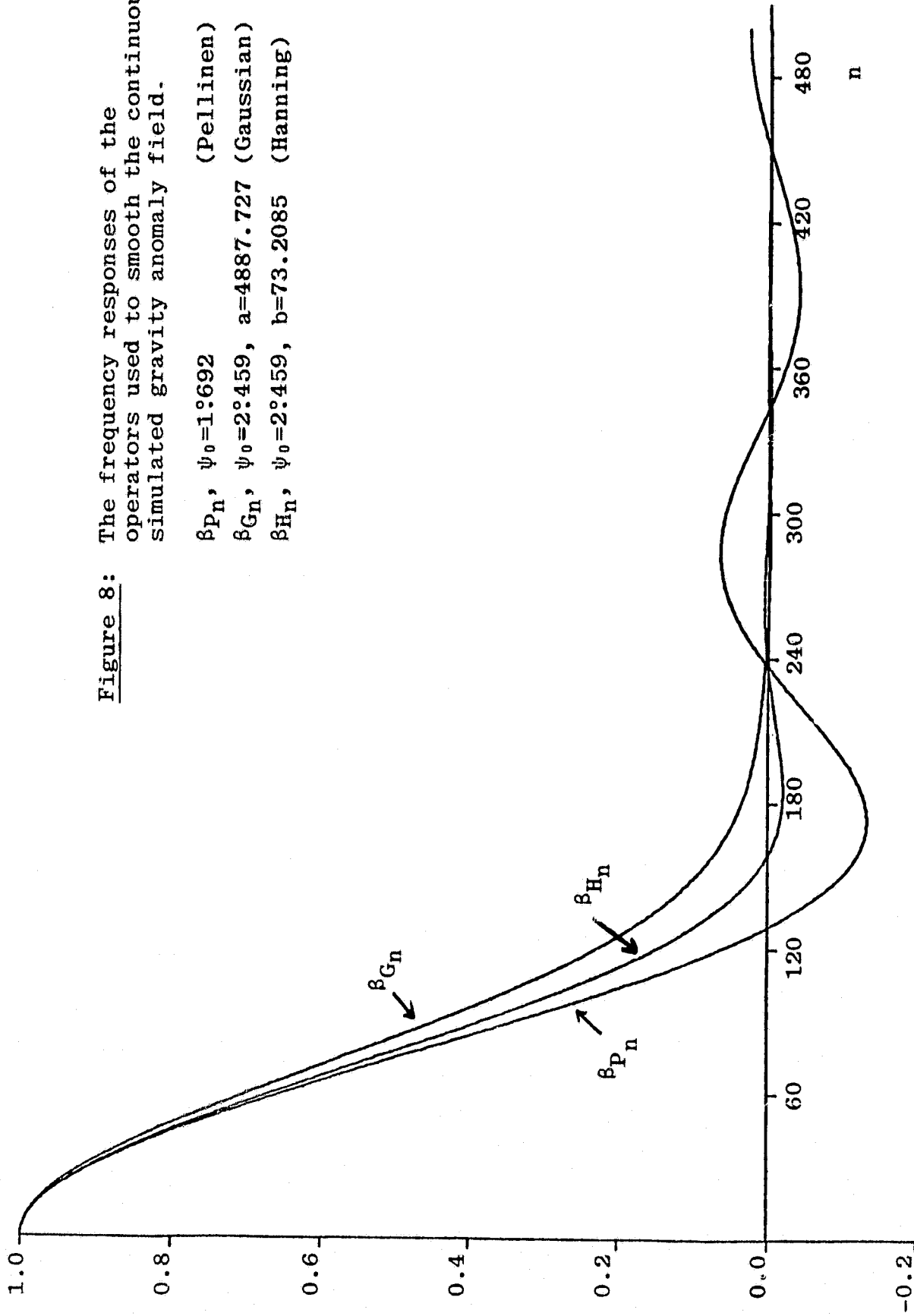
The averaging process, in the practical situation, is performed on discrete values of the point function. Consider the following discrete smoothing kernels

$$B_k(\psi_j) = \frac{w_k(\psi_j)}{\Omega_k(\psi_0)}, \quad k = P, G, H \quad (88)$$

*(where $\phi = 90^\circ - \theta$)

Figure 8: The frequency responses of the operators used to smooth the continuous simulated gravity anomaly field.

β_{P_n} , $\psi_0=1:692$ (Pellinen)
 β_{G_n} , $\psi_0=2:459$, $a=4887.727$ (Gaussian)
 β_{H_n} , $\psi_0=2:459$, $b=73.2085$ (Hanning)



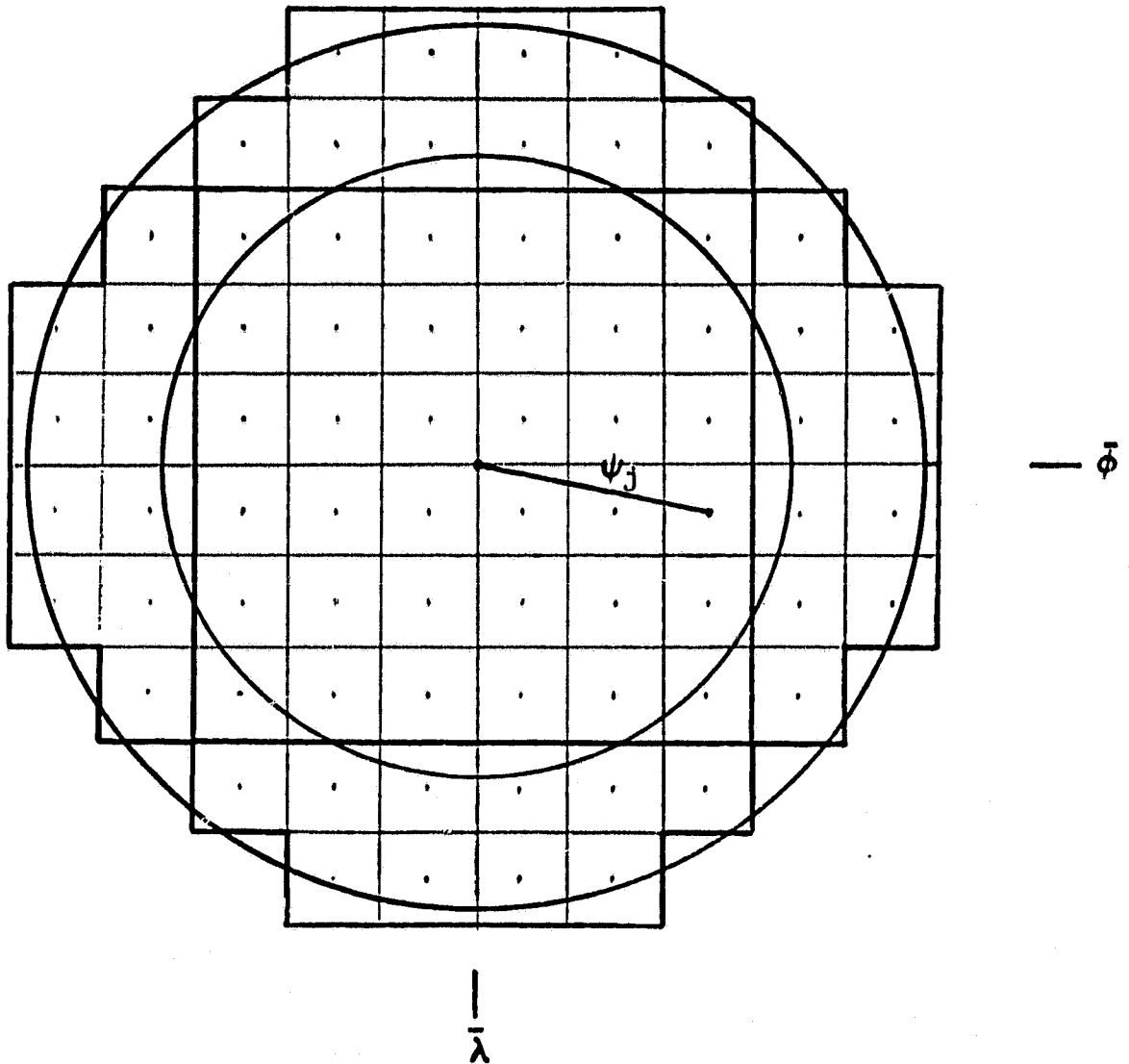


Figure 9: Spherical caps of radii $\psi_0=1:692$ and $\psi_0=2:459$ defined as having the area of 36 and 76 $0:5 \times 0:5$ blocks, respectively. For the simulation, the continuous function is averaged over the caps, and the discrete function is averaged over the block values.

$$\cos\psi_j = \sin\bar{\phi} \sin\phi_j + \cos\bar{\phi} \cos\phi_j \cos(\bar{\lambda} - \lambda_j)$$

$$\phi_{j+1} - \phi_j = \lambda_{j+1} - \lambda_j = 0:5$$

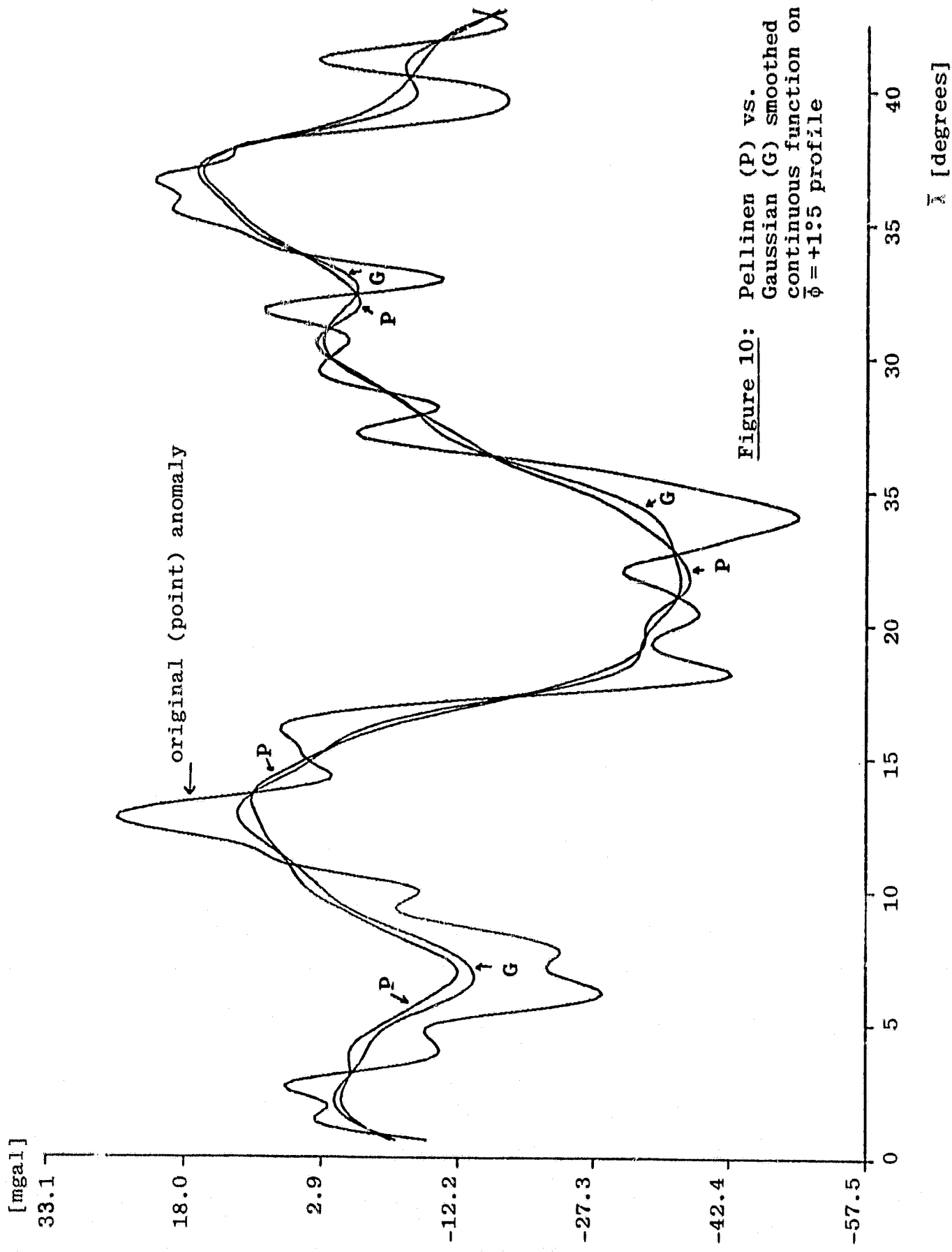
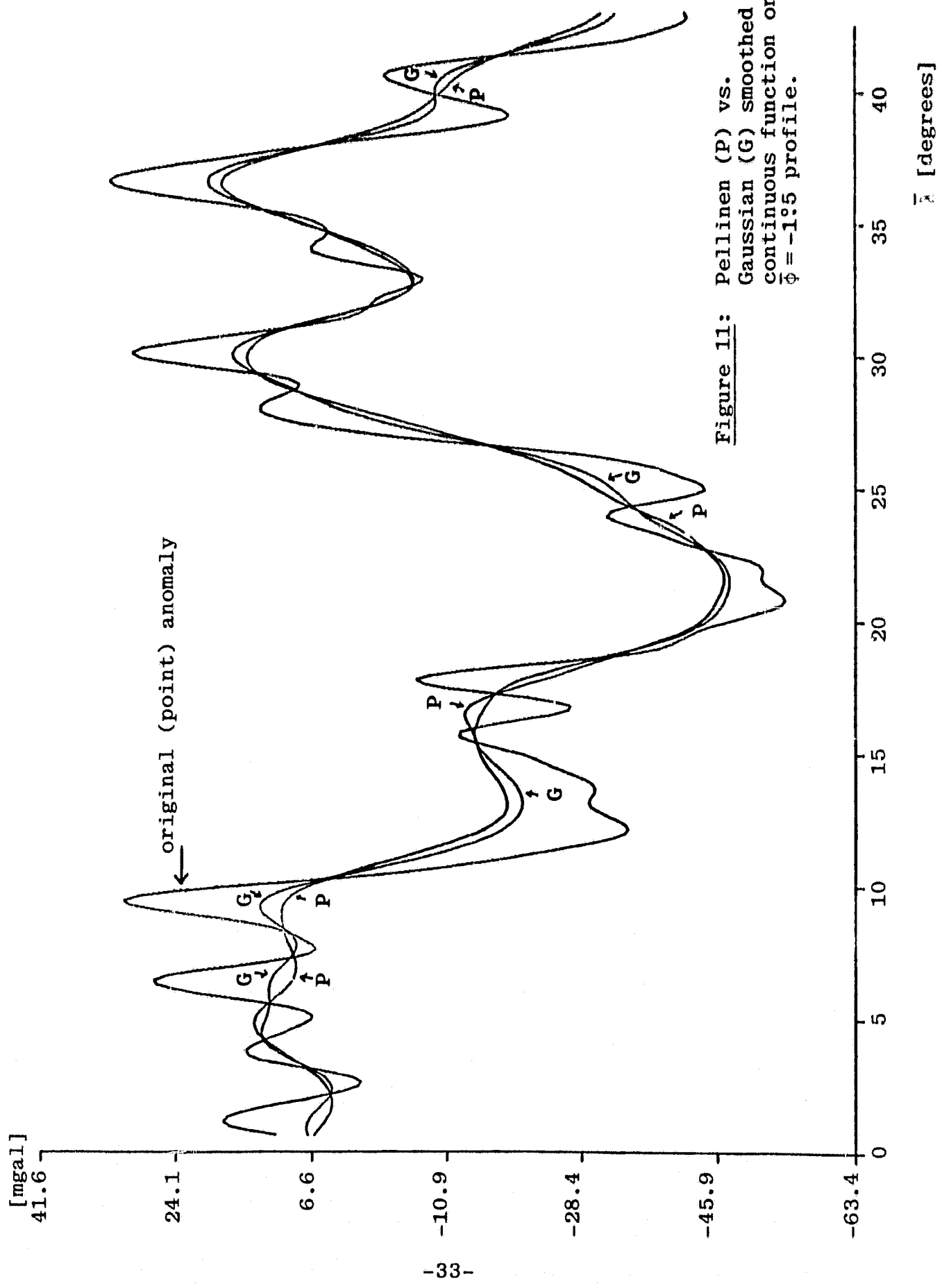


Figure 10: Pellinen (P) vs. Gaussian (G) smoothed continuous function on $\bar{\phi} = +1:5$ profile



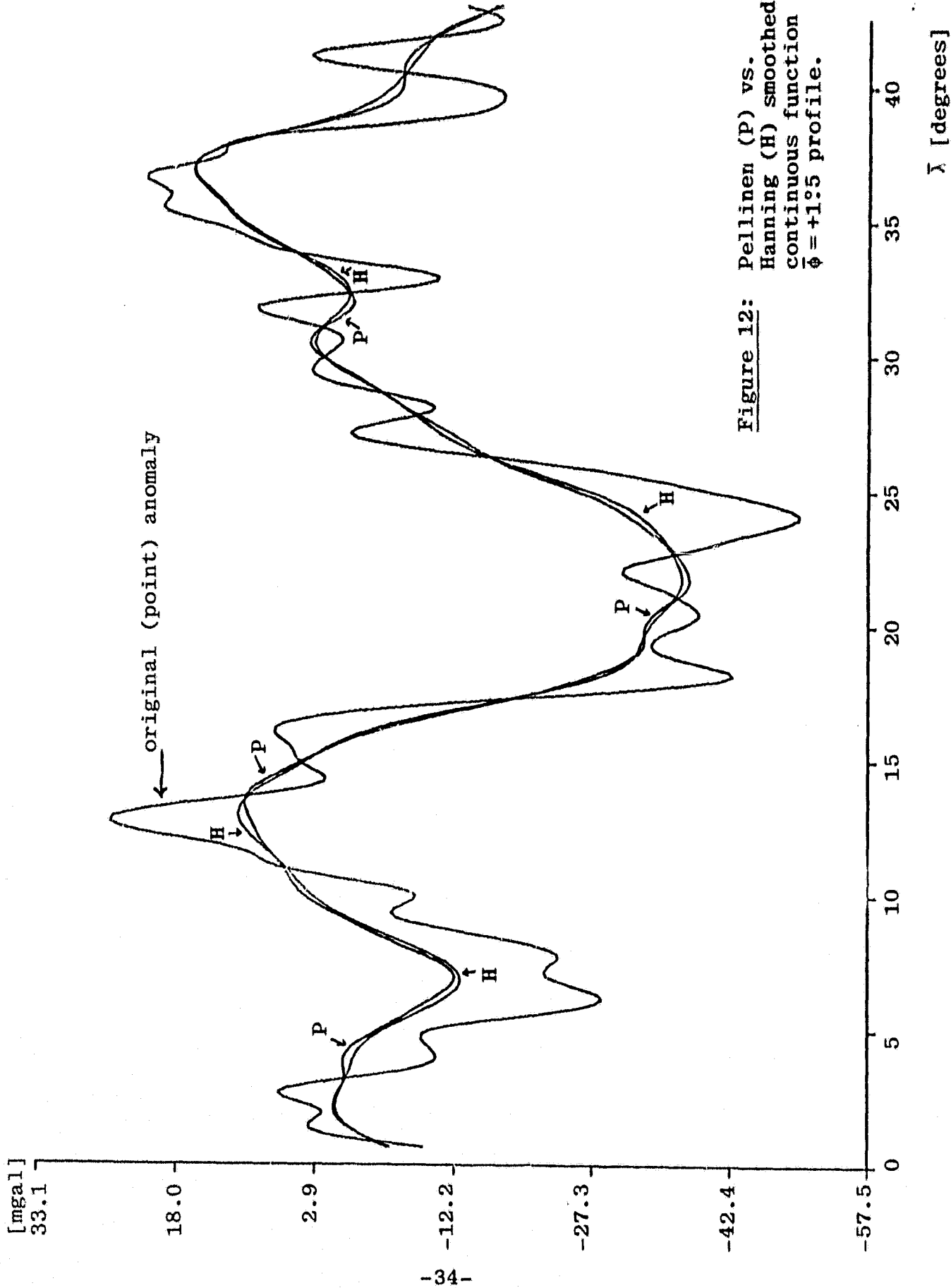


Figure 12: Pellinen (P) vs. Hanning (H) smoothed continuous function on $\phi = +1:5$ profile.

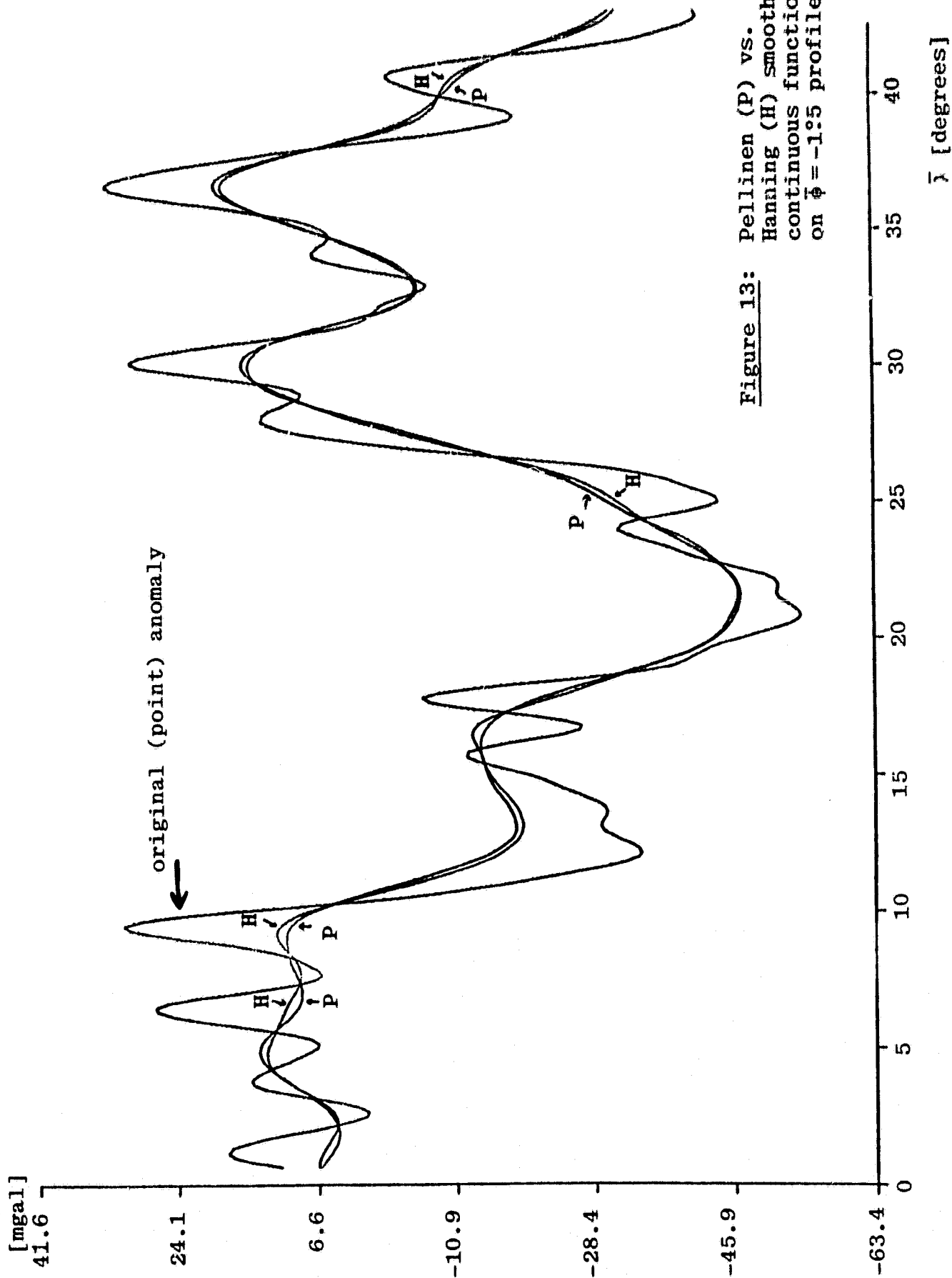


Figure 13: Pellinen (P) vs.
 Hanning (H) smoothed
 continuous function
 on $\phi = -1.5$ profile.

where

$$\Omega_k(\psi_0) = \frac{1}{4\pi} \sum_{j=1}^M w_k(\psi_j) \Delta\sigma_j \quad (89)$$

and $\Delta\sigma_j$ is the area of the block containing a known value of the point function. $\Omega_k(\psi_0)$ is the discretized integral of the weighting function over the cap (see (51)); and although, for the $w_k(\psi)$ considered here, these integrals are evaluable analytically, their discretization guarantees the unbiasedness of the averaging process

$$\text{(i.e. } \frac{1}{4\pi} \sum_{j=1}^M B_k(\psi_j) = 1\text{)}.$$

In order to simulate the process of averaging, the coefficients (86) were synthesized on a 0.5×0.5 grid in the equatorial region defined by $-3.75 \leq \phi \leq 3.75$, and $0.25 \leq \lambda \leq 42.75$. The Pellinen, Gaussian, and Hanning smoothing kernels were evaluated at ψ_j , $j=1, \dots, M_k$, where M_k is the number of 0.5×0.5 blocks in each of the caps (see Figure 9, $M_p = 36$, $M_G = M_H = 76$). Subsequently, the average gravity anomaly for each of the weighting functions (P,G,H) was computed on the profiles $\phi = \pm 1.5$, at 0.5 intervals, using equation (84). These "moving averages" are plotted against the original point function in Figures 14 and 15 (Pellinen vs. Gaussian averages) and Figures 16 and 17 (Pellinen vs. Hanning averages). We note that, although the frequency responses of the (discrete) operators are not precisely those of Figure 8, the averaging characteristics illustrated in these figures are essentially identical to those described for the continuous (isotropic) operators.

Normally, the equally weighted (Pellinen) average, in the example above, would be computed on a $3^\circ \times 3^\circ$ grid. The "polarity reversals" would then not be directly apparent. Also, if the errors of the original point data were statistically uncorrelated, so would be the errors in the 3° Pellinen means. The propagated errors in the Gaussian and Hanning averages, however, will be correlated if the caps are not disjoint. Figure 18 shows the possible configurations for the above example if the averages are computed on a $3^\circ \times 3^\circ$ grid. Each shaded region represents the overlap between two "caps" which is responsible for the correlation. Assuming that all point data have the same standard error σ with zero correlation, the correlation in the means is given by

$$\rho_k(A,B) = \frac{\sigma^2 \sum_{i=1}^{L_{AB}} q_k(A, j_i) q_k(B, j_i)}{\sigma_k(A) \sigma_k(B)} \quad (90)$$

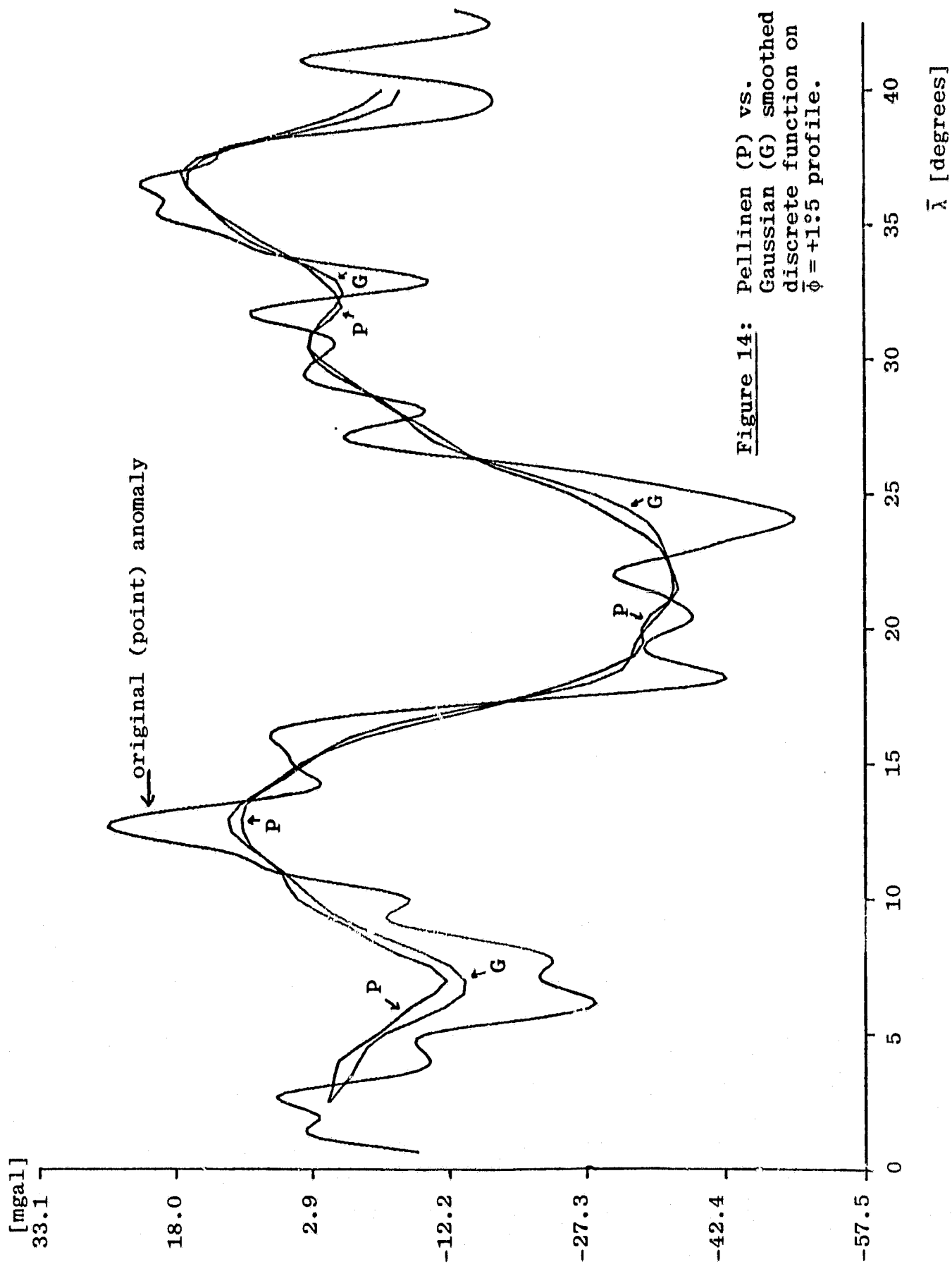


Figure 14: Pellinen (P) vs. Gaussian (G) smoothed discrete function on $\phi = +1:5$ profile.

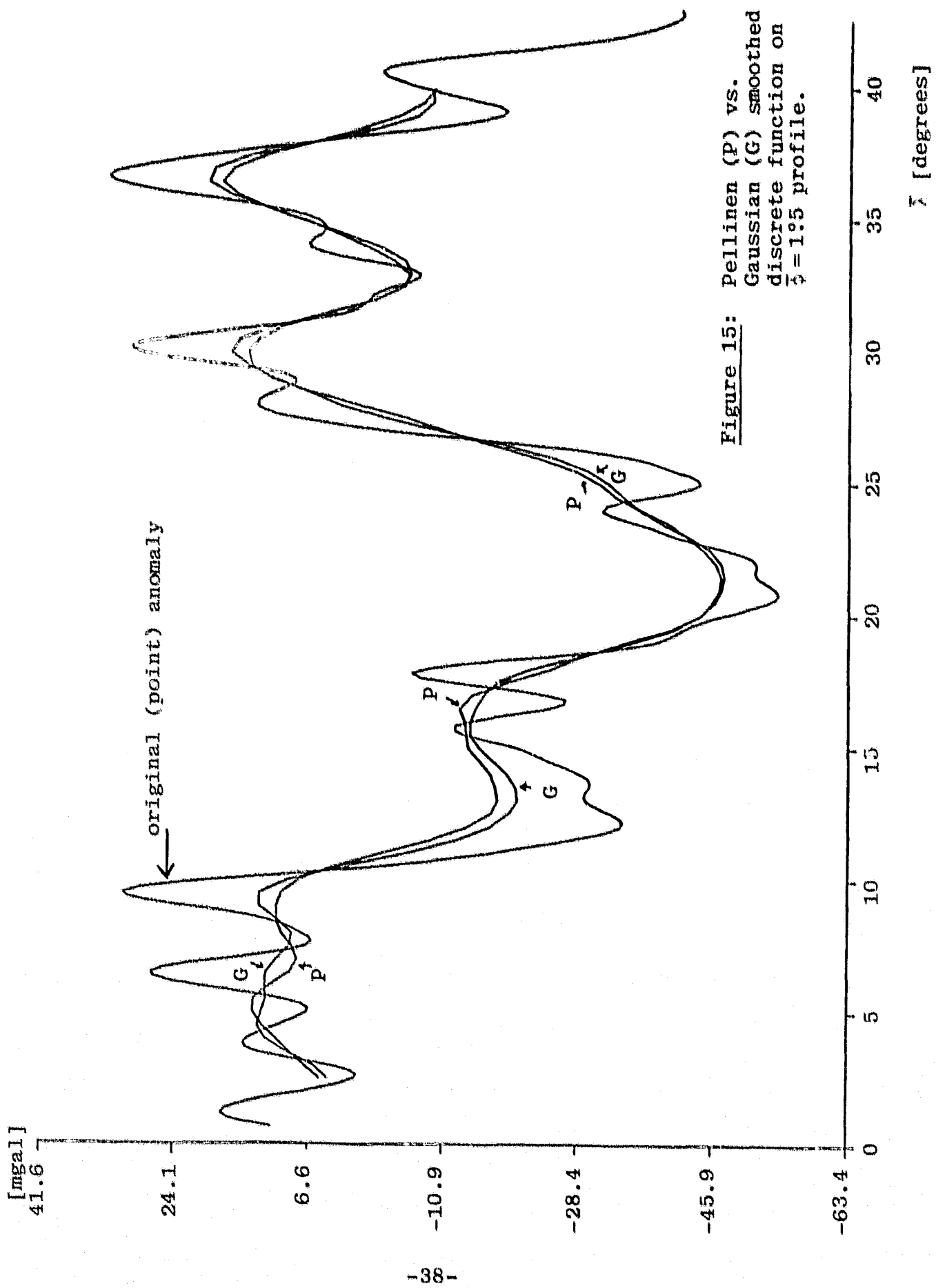


Figure 15: Pellinen (P) vs. Gaussian (G) smoothed discrete function on $\lambda = 1:5$ profile.

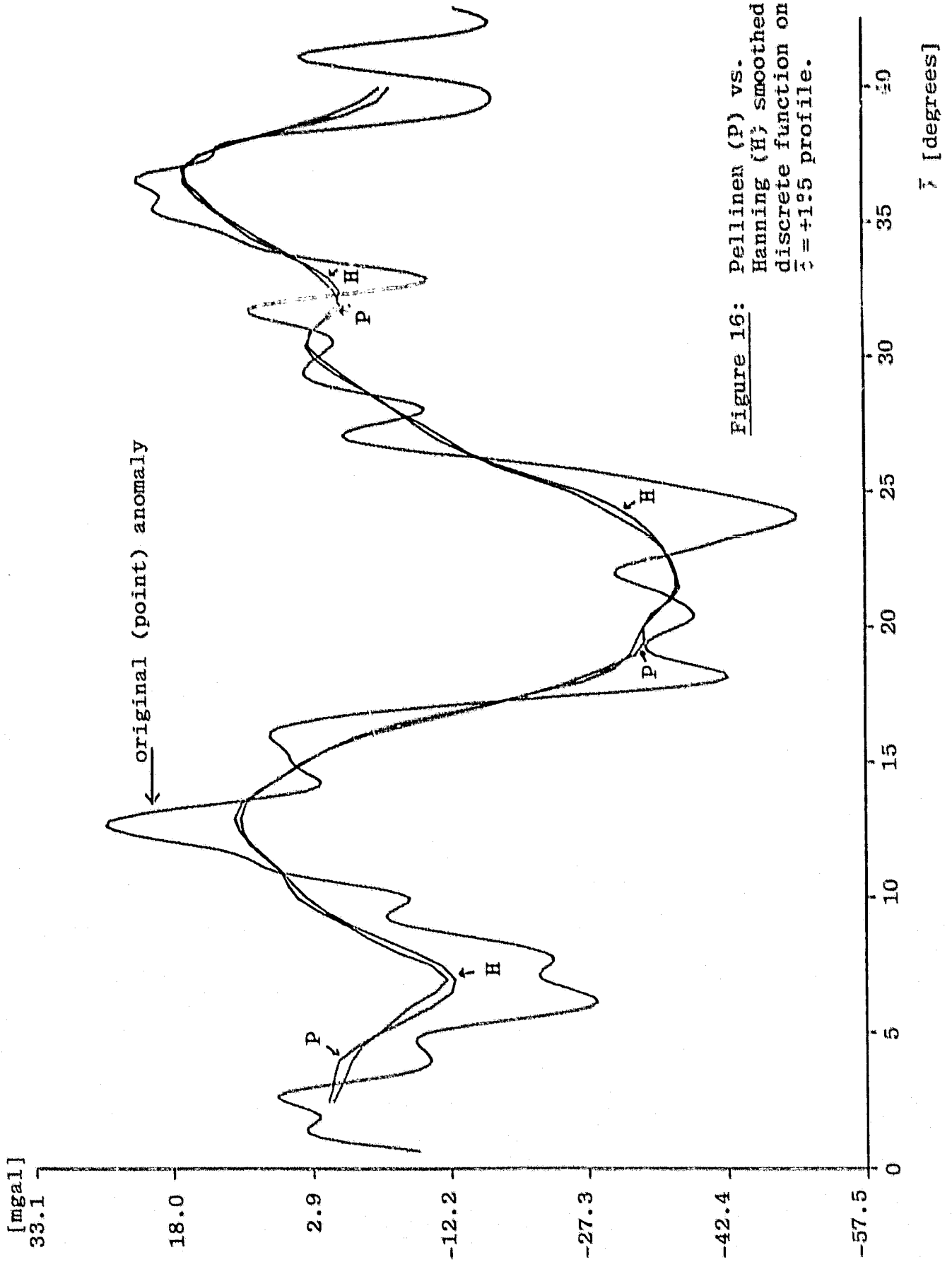
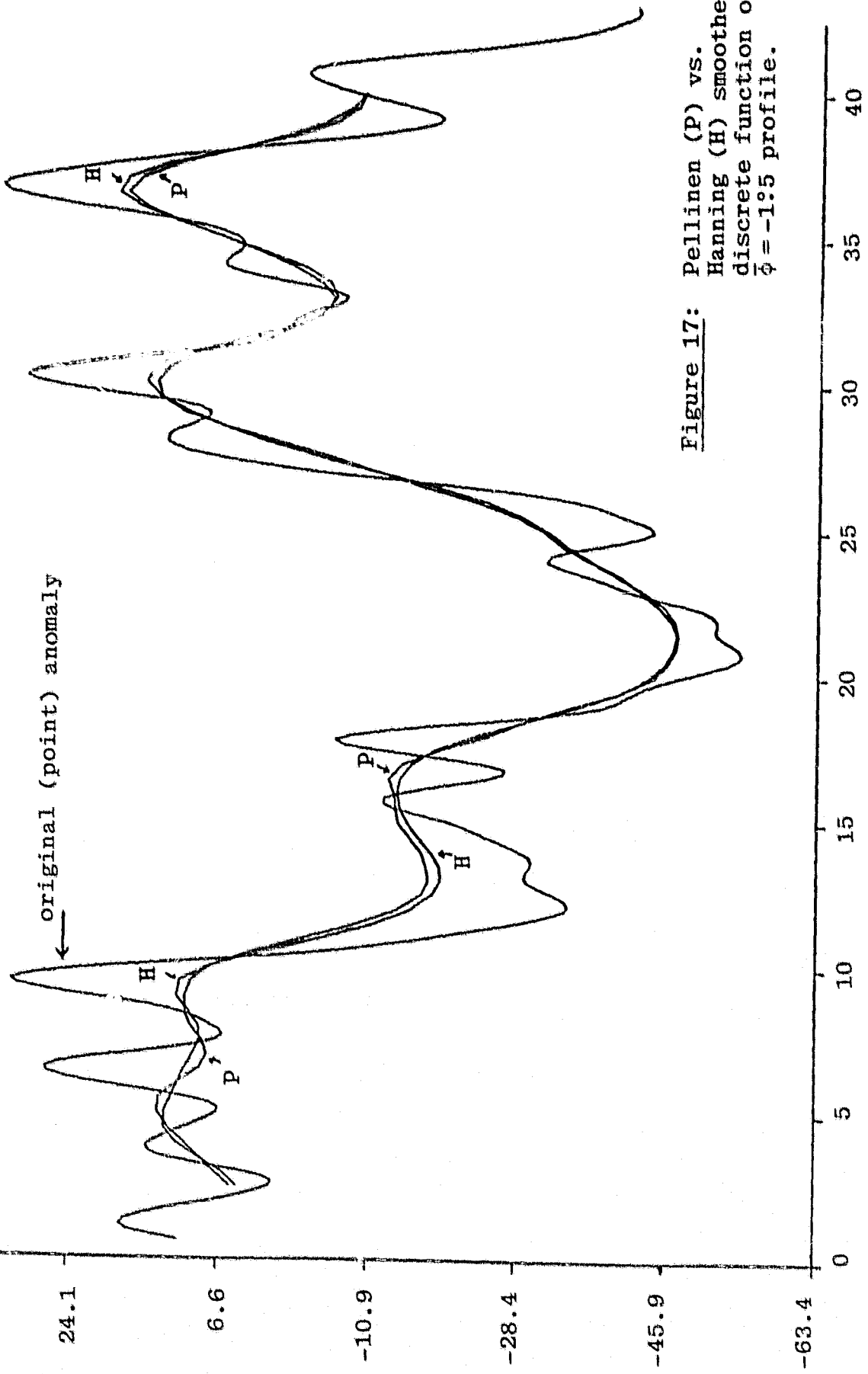


Figure 16: Pellinen (P) vs. Hanning (H) smoothed discrete function on $\bar{c} = +1.5$ profile.

[mgal]



original (point) anomaly

Figure 17: Pellinen (P) vs. Hanning (H) smoothed discrete function on $\bar{\phi} = -1:5$ profile.

λ [degrees]

where L_{AB} is the number of points j_i common to the two "caps", A and B (in Figure 18, $L_{AB} = 4$, $L_{AC} = 20$); and

$$q_k(A, j) = \frac{1}{4\pi} B_k(\psi_j) \Delta\sigma_j = \frac{w_k(\psi_{Aj}) \Delta\sigma_j}{4\pi \Omega_k(\psi_0)} \quad (91)$$

ψ_{Aj} being the central angle between the center of the "cap" A and the point j; and where

$$\sigma_k^2(A) = \sigma^2 \sum_{j=1}^M q_k(A, j) \quad (92)$$

If $\Delta\sigma_j$ and Ω_k are constant, then

$$\rho_k(A, B) = \frac{\sum_{i=1}^{L_{AB}} w_k(\psi_{Aji}) w_k(\psi_{Bji})}{\sum_{j=1}^M w_k^2(\psi_{Aj})} \quad (93)$$

With respect to Figure 18 and the above example

$$\begin{aligned} \rho_G(A, B) &= 3.0 \times 10^{-4} & , & & \rho_H(A, B) &= 2.3 \times 10^{-4} \\ \rho_G(A, C) &= 3.2 \times 10^{-2} & , & & \rho_H(A, C) &= 4.6 \times 10^{-2} \end{aligned} \quad (94)$$

These are generally not considered significant correlations.

5. Conclusion

From its birthplace in electrical engineering, the application of the spectral theory has spread to many unrelated disciplines, becoming indispensable in the methodical analysis of large amounts of data. In geodesy, while there is the complication of having to work on the sphere, many of the basic concepts of spectral theory are directly applicable, as in the study of smoothing operators. The effects of the different methods to smooth the gravity anomaly field can be properly assessed only by inspecting the spectrum of the corresponding weighting function. It is shown that the mean

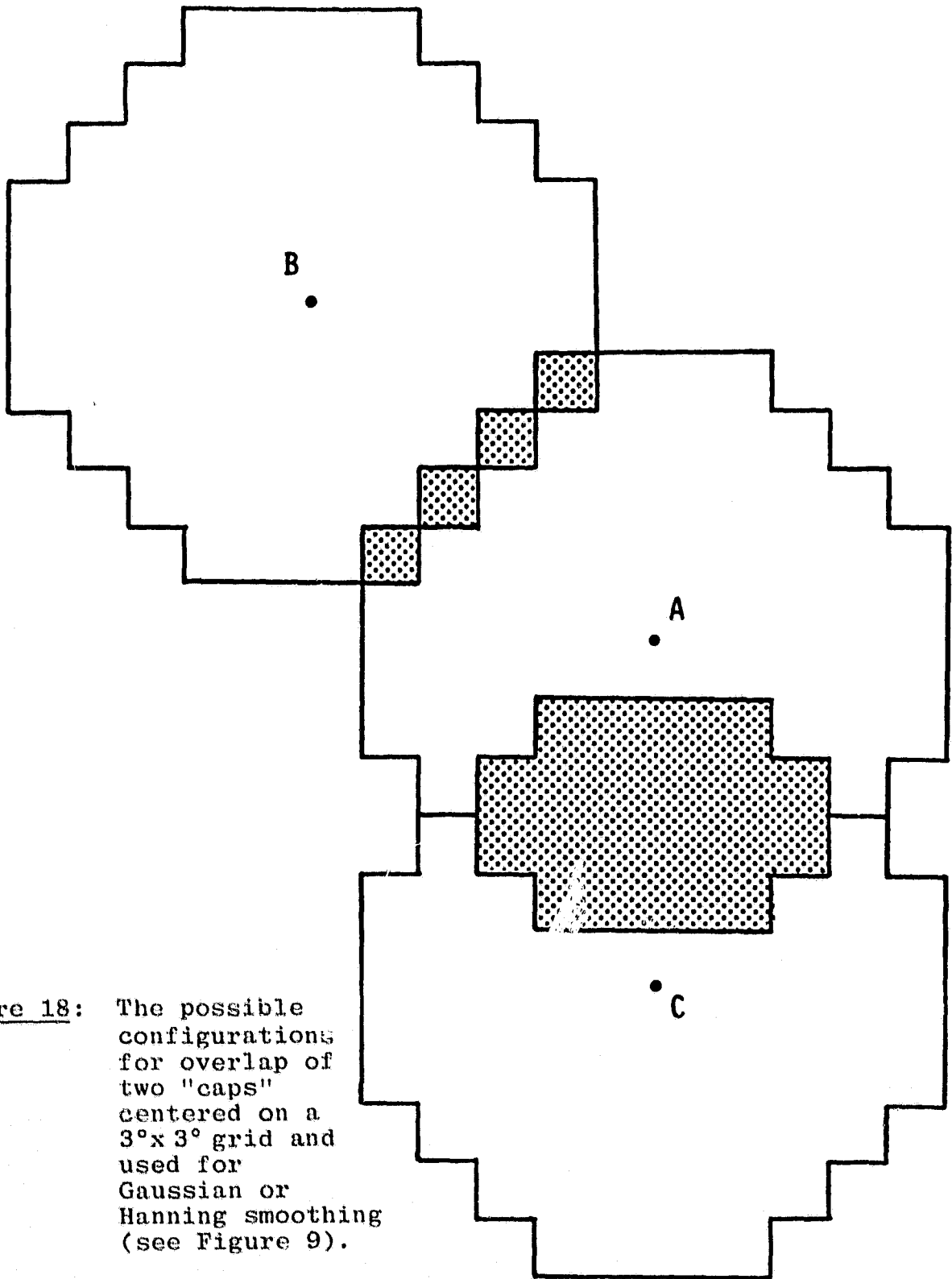


Figure 18: The possible configurations for overlap of two "caps" centered on a $3^\circ \times 3^\circ$ grid and used for Gaussian or Hanning smoothing (see Figure 9).

gravity anomaly acquires new and different connotations when various weighting schemes are introduced. By an example, we saw that the excursions of the Pellinen frequency response into the negative can cause 180° phase shifts in the smoothed function (see Figures 10-17). Furthermore, from Figures 4, 5 and 8 it is readily evident that both the Hanning and Gaussian smoothing operators (with a suitable choice of the parameter "a") do a better job of filtering the high-degree components from the total field than the Pellinen operator. Finally, it is noted that a truncated spherical harmonic series (e.g. $n_{\max} = 180$) cannot justifiably be characterized as a Pellinen, or other, mean function, unless the coefficients of the series are multiplied by the corresponding frequency response which, in addition, must have no significant components beyond degree n_{\max} .

References

- Bath, M., Spectral Analysis in Geophysics, Developments in Solid Earth Geophysics, Elsevier Scientific Publishing Company, Amsterdam, 1974.
- Breakwell, J., "Satellite Determination of Short Wavelength Gravity Variations," The Journal of the Astronomical Sciences, vol. 27, no. 4, Sept.-Dec. 1979.
- Churchill, R.V. and C.L. Dolph, "Inverse Transforms of Products of Legendre Transforms," Proc. Amer. Math. Soc., vol. 5, 1954.
- Cushing, J.T., Applied Analytical Mathematics for Physical Sciences, John Wiley and Sons, Inc., New York, 1975.
- Gaposchkin, E.M., "Averaging on the Surface of a Sphere," Journal of Geophysical Research, vol. 85, no. B6, June 10, 1980.
- Harris, F.J., "On the Use of Windows for Harmonic Analysis with the Discrete Fourier Transform," Proc. IEEE, vol. 66, no. 1, pp. 51-83, Jan. 1978.
- Heiskanen, W.A., and H. Moritz, Physical Geodesy, W.H. Freeman and Co., San Francisco, 1967.
- Hobson, E.W., The Theory of Spherical and Ellipsoidal Harmonics, reprint by Chelsea Publishing Company, New York, 1965.
- Holloway, J.L., "Smoothing and Filtering of Time Series and Space Fields," Advances in Geophysics, vol. 4, pp. 351-389, 1958.
- Jordan, S.K., "Fourier Physical Geodesy", report TIM-868-2, The Analytical Sciences Corporation, Reading, MA, 1978.
- Kaula, W.M., "Statistical and Harmonic Analysis of Gravity," Journal of Geophysical Research, vol. 65, no. 12, pp. 2401-2421, Dec. 1959.
- Kaula, W.M., "Theory of Statistical Analysis of Data Distributed over a Sphere", Reviews of Geophysics, vol. 5, no. 1, pp. 83-107, 1967.
- Kellogg, O.D., Foundations of Potential Theory, reprint by Dover Publications, Inc., New York, 1953.
- Krarpup, T., "A Contribution to the Mathematical Foundation of Physical Geodesy," Publ. no. 44, Danish Geodetic Institute, Copenhagen, 1969.

- Meissi, P.A., "A Study of Covariance Functions Related to the Earth's Disturbing Potential," report No. 151, Department of Geodetic Science, The Ohio State University, 1971.
- Moritz, H., "Methods for Downward Continuation of Gravity," report no. 67, Department of Geodetic Science, The Ohio State University, 1966.
- Müller, C., "Spherical Harmonics," Lecture Notes in Mathematics, ed. A. Dold and B. Eckmann, Springer-Verlag, Berlin, 1966.
- Papoulis, A., Signal Analysis, McGraw Hill Book Company, New York, 1977.
- Pellinen, L.P., "A Method for Expanding the Gravity Potential of the Earth in Spherical Harmonics", Translation ACIC-TC-1282, NTIS: AD-661819, Moscow, 1966.
- Pollack, H.N., "Spherical Harmonic Representation of the Gravitational Potential of a Point Mass, a Spherical Cap, and a Spherical Rectangle," Journal of Geophysical Research, Vol. 78, No. 11, pp. 1760-1768, 1973.
- Rapp, R.H., "The Relationship Between Mean Anomaly Block Sizes and Spherical Harmonics Representations," Journal of Geophysical Research, vol. 82, no. 33, pp. 5360-5364, 1977.
- Rapp, R.H., "A Global 1°x 1° Anomaly Field Combining Satellite, GEOS-3 Altimeter and Terrestrial Anomaly Data," report no. 278, Department of Geodetic Science, The Ohio State University, 1978.
- Rapp, R.H., "Potential Coefficient and Anomaly Degree Variance Modelling Revisited," Report No. 293, Department of Geodetic Science, The Ohio State University, 1979.
- Rayner, J.N., An Introduction to Spectral Analysis, Monographs in Spatial and Environmental System Analysis, Pion Limited, London, 1971.
- Robertson, W.M., "Spherical Geodetic Transformations, Spectral Theory and Optimal Template Design," vol. I, Report R-1181, The Charles Stark Draper Laboratory, Inc., Cambridge, MA, 1978.
- Sjöberg, L., "A Recurrence Relation for the β_n -Function," Bulletin Geodesique, vol. 54, no. 1, pp. 69-72, 1980.
- Wenzel, H.-G. and D. Arabelos, "Zur Schätzung von Anomalie-Gradvarianzen aus Lokalen Emperischen Kovarianzfunktionen," Zeitschrift für Vermessungswesen, vol. 106, no. 5, pp. 234-243, 1981.

Appendix A

Let

$$\gamma_n = \int_{y_0}^1 e^{ay} P_n(y) dy \quad (\text{A.1})$$

Substituting the relationship

$$(2n+1) P_n(y) = P'_{n+1}(y) - P'_{n-1}(y) \quad (\text{A.2})$$

where the primes denote differentiation with respect to y , into (A.1) and integrating by parts results in

$$\gamma_n = \frac{1}{2n+1} [e^{ay_0} (P_{n-1}(y_0) - P_{n+1}(y_0)) - a(\gamma_{n+1} - \gamma_{n-1})] \quad (\text{A.3})$$

Equation (65) follows upon realizing that, with $y = \cos\psi$, $y_0 = \cos\psi_0$,

$$\begin{aligned} \tilde{\beta}_{Gn} &= \frac{\tilde{b}_{Gn}}{\sqrt{2n+1}} = \frac{1}{\int_{y_0}^1 e^{-a(1-y)} dy} \int_{y_0}^1 e^{-a(1-y)} P_n(y) dy \\ &= \frac{ae^{-a}}{1 - e^{-a(1-y_0)}} \gamma_n \end{aligned} \quad (\text{A.4})$$

Appendix B

Let

$$\alpha_n = \int_0^{\psi_0} \cos b\psi P_n(\cos\psi) \sin\psi \, d\psi \quad (\text{B.1})$$

Substituting (A.2) into (B.1) and integrating by parts yields

$$\alpha_n = D_n + \frac{b}{2n+1} (\delta_{n-1} - \delta_{n+1}) \quad (\text{B.2})$$

where

$$D_n = \frac{\cos b\psi_0}{2n+1} [P_{n-1}(\cos\psi_0) - P_{n+1}(\cos\psi_0)] \quad (\text{B.3})$$

and

$$\delta_n = \int_0^{\psi_0} \sin b\psi P_n(\cos\psi) \sin\psi \, d\psi \quad (\text{B.4})$$

Now from (Hobson, 1965, pp. 32-33),

$$\frac{1}{n}(1-y^2) P'_n(y) = \frac{n+1}{2n+1} (P_{n-1}(y) - P_{n+1}(y)) \quad (\text{B.5})$$

Hence

$$\frac{n+1}{2n+1} (\delta_{n-1} - \delta_{n+1}) = \frac{-1}{n} \int_0^{\psi_0} \sin b\psi \sin\psi \frac{d}{d\psi} P_n(\cos\psi) d\psi \quad (\text{B.6})$$

Again, integrating by parts, we obtain

$$\begin{aligned} \frac{n+1}{2n+1} (\delta_{n-1} - \delta_{n+1}) = \\ - \frac{1}{n} E_n + \frac{1}{n} \int_0^{\psi_0} \sin b\psi \cos\psi P_n(\cos\psi) \sin\psi \, d\psi + \frac{b}{n} \alpha_n, \end{aligned} \quad (\text{B.7})$$

which, upon substituting $(n+1) P_{n+1}(y) + nP_{n-1}(y) = (2n+1)yP_n(y)$, as well as (B.2), gives after several manipulations

$$\frac{(n+1)^2 - b^2}{2n+1} \delta_{n+1} - \frac{n^2 - b^2}{2n+1} \delta_{n-1} = E_n - bD_n \quad (\text{B.8})$$

where

$$E_n = \sin b\psi_0 \sin\psi_0 P_n(\cos\psi_0) \quad (\text{B.9})$$

Equation (B.8) can be reformulated as

$$\delta_{n-1} - \delta_{n+1} = \frac{2n+1}{n^2 - b^2} (\delta_{n+1} - E_n + bD_n) \quad (\text{B.10})$$

Combining this with (B.2), we have

$$(n^2 - b^2)\alpha_n = n^2 D_n + b\delta_{n+1} - bE_n \quad (\text{B.11})$$

and

$$[(n-2)^2 - b^2]\alpha_{n-2} = (n-2)^2 D_{n-2} + b\delta_{n-1} - bE_{n-2} \quad (\text{B.12})$$

The δ_n 's are eliminated by subtracting (B.12) from (B.11) and substituting (B.10). This results in

$$\begin{aligned} [(n+1)^2 - b^2]\alpha_n &= [(n-2)^2 - b^2]\alpha_{n-2} + (n+1)^2 D_n - (n-2)^2 D_{n-2} + \\ &\quad -b(E_n - E_{n-2}) \end{aligned} \quad (\text{B.13})$$

thus proving equation (75).